NAL PROPOSAL NO. 614

Scientific Spokesman:

J. Rosen
Northwestern University
Department of Physics and
Astronomy
Evanston, Illinois 60201

Comm: 312-492-5457

Study of High Mass Multiphoton States and Direct Photon Production

Northwestern University

Notre Dame University

Carnegie Mellon University

Fermilab

October 1978

October 1978

Proposal

Study of High Mass Multiphoton States and Direct Photon Production

Northwestern, Notre Dame, Carnegie Mellon, Fermilab Collaboration

Spokesman:

J. Rosen

Northwestern University

I. Introduction

The motivation for undertaking the study of direct single and multiple photon production in hadronic collisions is well known and requires little comment or justification[1-6]. We are all aware of the enormous activity in the related area of direct lepton production. This effort has been rewarded with a richness of physics relating to both continuum production mechanisms and resonant states (ρ, ω, ϕ, ψ's, Υ's). Direct photon studies should both overlap and complement this lepton physics. One can study the single and double photon continuum and look for resonant states -- most notably η_c, $\eta_B \rightarrow \gamma + \gamma$.

Why has photon production physics not flourished? Again, the nature of the difficulties is clear. Good spatial and energy resolution coupled with the ability to separate π^0 and η^0 derived photons is required. Other accompanying final state hadrons do not help the situation either, but the π^0 remains as the single most formidable obstacle. We believe that a large area, finely sectorized liquid Argon shower calorimeter constitutes the best tool for achieving $\gtrsim$ 2 orders magnitude improvement in sensitivity relative to what has been acheived to date[7,8].

Our collaboration is currently setting up E-515 in the M1 beam of the Meson Laboratory. We anticipate the initiation of experimentation in the post Mesopause period starting in March 1979. Figures 1 and 2 display plan and elevation views of the spectrometer system. The

most significant detector system for the purposes of the present considerations is the shower calorimeter positioned just downstream of the multicell Cerenkov counter. The shower detector plays two roles in the context of E-515.

(1) Momentum analyzed electrons and hadrons will be separated on the basis of pulse height in order to establish the yield of $\mu^{\pm} e^{\mp}$ events. These events are circumstantially interpreted to result from the associated production of short lived hadrons (presumably charm) and their subsequent semileptonic decay.

(2) γ, π^o, η^o,... components of explicit charm particle hadronic modes will be recorded.

Role (2) is the more demanding of the two. One of our earliest goals will be to bring this system into operation, populate the bulk of the detector with γ's and record sufficient data to provide calibration and a basis for software pattern recognition development. This will be executed with the aid of an auxiliary target and trigger definition quite apart from that of E-515. The strategy is quite simple. We want high $P_\perp$ γ's to populate the body of the detector. Initially, we wish to avoid an overlay of charged hadron "hits" on the detector. This is easily done with veto counters. After we have mastered neutral final states we will contemplate neutrals plus charged particles which require external tracking. The testing and software development of the charged particle chamber system will be decoupled from the shower detector.

The outlined program is logical and necessary to the goals of E-515. We shall attempt to demonstrate in this proposal that our new detector is the best device at Fermilab for assaying high $P_\perp$ γ production. To achieve even our initial modest and exploratory goals will undoubtedly

require a block of running time significantly beyond that envisaged for a minimum systems check.

Fermilab and the Program Advisory Committee should be aware of our capabilities and thinking. We welcome comments and criticisms and look forward to some degree of endorsement.

What advantages do we have relative to earlier ISR experiments on direct photon production?

We can target pions as well as protons.

Our luminosity and acceptance are significantly larger.

Although our CM energy is lower, our ability to separate π^o and η^o produced γ's from single γ's is superior. At Fermilab, γ_{CM} is 10-15. The probability of failing to detect the weaker of a pair of γ's is tional to 1/E. Our γ's are over an order of magnitude more energetic. Further, energy resolution goes like $E^{-\frac{1}{2}}$. The advantage for multi-photon studies is even more pronounced.

Why is our detector superior to a Pb glass wall?

The loss of weak γ's (which simultaneously correlate with larger π^o opening angle) is one side of the coin. A coarsely sectorized detector confronts the problem of resolving closely spaced, relatively symmetric γ pairs. Most Pb glass walls with comparable detection area employ with ~15 cm dimension. Our strip size is 1.25 cm.

Sometimes external converters are used with Pb glass walls and some kind of PWC or hodoscope arrangement is used to fine sectorize the coordinate. But then the coordinates are given by pulses with little or no sensitivity to the primary energy. Such systems are prone to register many false or low energy "hits". This is particularly irksome when confronting high multiplicity high energy physics.

The liquid argon system is of course, slower. The double pulse resolving time of the elements is 200-250ns.

Some comments on other detector systems with similar sectorization.

The pioneering prototype x,y sectorized detector is that prepared by Tollestrup, Walker and coworkers. This detector featured 0.5 m^2 area, 70x70 cells and a Pb, scintillator lattice. An extremely clever arrangement for light collection position compensation was employed. The basic moment analysis scheme described in section III was first worked out by this group. We assume the reader is familiar with the very fine low cross section measurements of explicit π^o and η^o production recorded with this detector. Our detector has a significantly larger area and number of cells and has finer sampling. Although the liquid Argon system is an order of magnitude slower in double pulse resolving time, we believe that the large beam hole built into our system will preclude pile up and associated problems which are a consequence of beam particles and low $P_\perp$ secondaries.

The Rochester liquid Argon system which has undergone successful initial operation is similar to ours. Our system has comparable gap spacing and sampling, 3x the area, more cells (384 vs. 240) and a large beam hole. Our detector was designed explicitly for large mass, low cross section, small x physics.

II. Description of the Liquid Argon Shower Counter.

The active region of the detector will be 1.2m high by 2.4m wide. It will be partitioned into identical left and right halves each 1.2m x 1.2m having separate vertical and horizontal sectorization. The detector will consist of a matrix of Pb sheets, etched printed circuit boards (G-10 base) and gaps filled with liquid argon.

The sequence will be

1. 3mm Pb sheet (+High Voltage)
2. 2mm Argon gap
3. Horizontal collection strips defining (96) 1.25cm cells on a 0.75mm thick printed circuit board. A low density pattern of nylon spacers will maintain the 2mm Argon gap on either side.
4. 2mm thick Argon gap
5. 0.75mm thick + High Voltage plane
6. 2mm thick Argon gap
7. Vertical collection strips (as in 3.)
8. 2mm thick Argon gap

Sum = 3mm Pb + 2.3mm G-10 board + 8mm of Argon = 13.3mm net.

The above sequence will repeat 28 times and constitute 20 radiation lengths of shower detector.

Obviously not all 2x2x28x96 = 12,288 strips will be separately read out electronically. The 28 layers in depth will be grouped into the (sum of) the first 14 and the last 14. Consequently, 768 channels of amplification pulse shaping, gating and ADC readout will be required.

There is a 12 cm diameter beam hole in the horizontal center and located 1/3 of the way down from the top. The liquid Argon is excluded from this hole by a cylindrical mylar cup containing helium gas. Figures 3 and 4 are photographs of the cathode plane art work. In the normal E-515 geometry the detection area subtends --

+32mr, -64mr (vertically)

$\pm$96mr (horizontally)

Recall that 90° in the CM corresponds to 70 mr (400 GeV) and 100mr (200 GeV). Hence the detector subtends a large fraction of the forward hemisphere in the CM. For the purposes of the neutral studies described in this proposal we will reduce the target - detector separation by approximately 2/3. The detector will then subtend

+50mr, -100mr (vertically)

$\pm$150mr (horizontally)

The beam hole will then correspond to a cavity with a cone half angle of 7.5 mr.

(The reason that the beam hole is located asymmetrically is that a portion of the upper half plane is reserved for and intercepted by the muon trigger system).

The Notre Dame group owns 80 Pb glass blocks $(3.5\text{in.})^2$ and 15 r.l. deep. These can be deployed in a matrix 16(H) x 5(V) just upstream of the detector. They would not play a role in the trigger but they would register π^{o} derived γ's and could improve the efficiency of direct γ isolation for those γ's which are recorded near the top of the liquid Argon detector. The Monte Carlo calculation of γ/π^{o} separation discussed later does <u>not</u> presume the existance of this supplementary wall.

The electronic readout system is basically identical to that provided by T. Droege for E-272. Relatively minor improvements are being made. Pulse rise time is dictated by the time required for electrons to drift across 2mm of liquid argon. The addition of methane helps speed the drift. The double pulse resolution is 200-250ns. This is consonant with efficient operation up to 10^6 interactions per pulse.

The cryogenic system is rather straightforward. Liquid nitrogen is the refrigerant and the steady state loss rate will be several hundred liters/day. The initial cool down and liquifaction of Argon that has passed through a purifier will be significantly higher. An auxilliary low heat loss buffer storage vessel exists.

Thermal insulation is provided by urethane insulation 9" thick. The incident γ's traverse $\frac{1}{2}$" thickness of press board, 9" of urethane and 3/16" of stainless steel. Given the size of our detector the wall thickness cannot sustain an internal vacuum. The wall forces would be several hundred thousand pounds. It is necessary to carefully purge the vessel interior in order to remove residual oxygen, the principal objectional contaminant. This procedure has proved to be satisfactory in the operation of a test vessel. Purging is practical but is admittedly a nuisance. The E-272 detector can be evacuated. We note this point because the E-272 detector which has already undergone successful operation, is virtually identical in all other essential aspects.

III. Multiphoton Kinematics and Trigger Definition

Consider a jet like cluster of particles with m_i^2, $(\vec{p}_{\perp i})^2 \gg P_i^2$. Neglecting higher order terms (m_i^4/p_i^4 etc.) the following useful formula can be readily derived.

(1) $$\frac{M^2 + (\vec{P}_\perp)^2}{P} = \sum_{i=1}^{n} \frac{m_i^2 + (\vec{P}_{\perp i})^2}{p_i}$$

where $\vec{P}_\perp = \Sigma \vec{p}_{\perp i}$, $P = \Sigma p_i$

Let us first examine the special case of a multiphoton system ($m_i^2 = 0$) and explicitly introduce the photon direction cosines α_i, β_i.

$$P_\perp^x = \Sigma p_{\perp i}^x = \Sigma \alpha_i p_i$$

$$P_\perp^y = \Sigma p_{\perp i}^y = \Sigma \beta_i p_i$$

It follows then that

(2) $$M^2(\text{multiphoton}) = (\Sigma \epsilon_i)(\Sigma \alpha_i^2 \epsilon_i + \Sigma \beta_i^2 \epsilon_i) - (\Sigma \alpha_i \epsilon_i)^2 - (\Sigma \beta_i \epsilon_i)^2$$

Suppose the multiphoton system is intercepted and recorded by our x,y sectorized liquid argon shower calorimeter. It is easy to see that the sum over discrete photons can be written as a sum over strip elements. Further, the small extant of shower spreading will produce a trivial amount of total mass increase. In effect, the experimental registration of the showers adds a very small, known effective mass to the photons. A small correction could be made using formula (1). Note that the mass (M) is established without requiring the matching of the x and y projections of the photons.

Formula (2) consists of several sums over strips elements. The direction cosines α_i, β_i are linearly related to the strip number. Hence the invariant mass M is given by a simple algebraic function of distribution moments. Let

$$V_n^x \equiv \Sigma(\alpha_i)^n \epsilon_i, \quad V_n^y \equiv \Sigma(\beta_i)^n \epsilon_i$$

then

$$M^2 = V_o(V_2^x + V_2^y) - (V_1^x)^2 - (V_1^y)^2$$

These moments can be generated in analogue voltage form (pulses) by simple linear addition of the fast outputs provided by the shower system electronics. This is accomplished by linearly summing fast output current pulses which are programmed by resistors with conductances proportional to α_i, α_i^2, etc. The quantity M^2 can be calculated in less than 200 ns by using commercially available 8 bit flash digitizers feeding into digital arithmetic elements. A threshold can be digitally set. In short a mass trigger can be generated without too much trouble. A $P_\perp$ trigger is even easier.

The front half of the detector has 384 elements. We will use only the front half for trigger purposes. Approximately 90% of the energy is deposited in the front half. Fast outputs which are the sums of adjacent groups of 4 will be used, hence we will be manipulating 4 groups of 16 outputs for trigger purposes. In all, 96 outputs will be cabled to the analogue summing matrices which are the front end of the trigger developing circuitry.

We will initiate our studies using a mass threshold $\sim$2.3 GeV/c^2 and a partially neutral final state requirement. This latter condition

which is fairly novel, requires some explanation. A totally neutral final state requirement seems highly restrictive. We will tolerate leading particles or low $p_\perp$ hadrons to traverse the central hole which subtends a half angle of 7.5 mr. A charged hadron with $p_\perp \gtrsim 0.5$ GeV/c and $p \geq 67$ GeV/c will satisfy this requirement. The veto counter which shadows the detector will contain a hole and is to be located part way between the detector and the target. It need not be particularly large and will not be larger than necessary so as to avoid intercepting large angle target fragments.

Past experience with hadron dynamics would seem to suggest that inclusive production of high mass states such as η_c should be orders of magnitude higher in cross section than explicit 2 body production at Fermilab energies.

We will search for η_c and other resonances decaying into $\gamma + \gamma$, and try to isolate the 1γ and 2γ continuum. A large number of conventional hadrons with neutral decay modes are expected to appear. A myriad of inclusive spectra and mass plots of various combinations are possible.

IV. High Mass Multiphoton States

We have estimated our acceptance for high mass diphoton states using a Monte Carlo with ψ-like production dynamics. Our acceptance for 2γ states is ~50% and remains flat to a mass of 10 GeV. Our apparatus subtends more than half of the solid angle in the CM.

Assuming 10^6 interactions/pulse we expect:

1 event/pulse/70nb

Using the data of on $\pi^+ \pi^-$ inclusive production (Kephart et. al.) and integrating their cross section over y and $P_\perp$, we infer:

$$\sigma(2\pi^o;\ M_{\pi^o\pi^o} \geq 2.3\ \text{GeV}) = 4\text{x}10^{-28}\text{cm}^2$$

Guessing that $\eta^o\pi^o$, $3\pi^o$, etc. will perhaps double this, a mass trigger threshold of 2.3 GeV by itself would yield 10^4 triggers/pulse. We really don't know how much the partial neutral final state restriction described in the previous section will depress this rate. We assume that the (trigger blocked) ratio $\gamma\gamma/\pi^o\pi^o$ is independent of the additional trigger restriction.

An experiment with 10^7 triggers would require ~100 hours ($3\text{x}10^4$ pulses). Assuming a mass resolution, σ mass $\sim(2\%)(3\text{GeV}) \simeq 60$ MeV off line analysis will yield:

$$\int_{2.8\ \text{GeV}}^{2.9\ \text{GeV}} \frac{d\sigma(\pi^o\pi^o)}{dm}\ dm = 5 \times 10^{-30}\text{cm}^2 \rightarrow 6 \times 10^4 \text{ events}$$

Assuming $\pi^o\pi^o$ rejection equal to $(.03)^2 = 10^{-3}$ (see section V) 2π's will simulate $\gamma\gamma$ and correspond to 60 background events. A 5σ signal will correspond to 40 events so that we will be sensitive to a cross section:

$$\sigma_{\eta_c \to \gamma\gamma} = \left(\frac{40}{60}\right)\left(10^{-3}\right) 5\times10^{-30} cm^2 = 4nb$$

The <u>exclusive</u> cross section for $\pi^- P \to n\gamma\gamma(\eta_c)$ reported CERN-USSR is 0.2nb. We expect that the inclusive cross section might be several orders of magnitude higher.

It is a relatively easy matter to discriminate against high γ multiplicity in the trigger. (It is easier than developing moments). It would be tantamount to requiring explicit η_c production outside of the central cone (described earlier). But then who knows? The higher multiplicity data may contain surprises of it's own. Our sensitivity to channels like

$$\eta_c \to \omega^o\omega^o(\omega^o \to \pi^o\gamma)$$

is non trivial.

V. High $P_\perp$ Direct Photon Production

For these studies one uses a $P_\perp$ threshold trigger. Our geometric detection efficiency is high ~70% and independent of $P_\perp$ up to ~9GeV/c. We expect:

1 event/pulse/40nb

using the π^- production data of Cronin et. al.[9], we infer:

$$\sigma(\pi^o,\ p_\perp > 3\ \text{GeV/c}) \simeq 2.5 \times 10^{-31}\text{cm}^2$$

This cross section drops by about a factor of 20 for each additional GeV/c increase in $P_\perp$. No data exists on high $P_\perp$ multineutral jets (i.e. the ratio π^o/neutral jet) so we don't know quantitativly, where the trigger $P_\perp$ threshold should be set to avoid saturation. There must be some available threshold and we guess that it is in the vicinity of 3-4 GeV/c.

We would like to carry out this study without any neutral requirement in the trigger. We would then like the charged hits in the shower detector to be registered by the downstream PWC system. More than half of the charged hadrons will pass through the first half of the shower detector registering only as minimum ionizing particles (~45 MeV). Those that interact will in general deposit only a small portion of their energy, typically a few hundred MeV. The charged hadrons should not compromise the trigger. They should be tagged however, so that candidate direct γ's are not confronted with a large number of apparent soft γ's which might accidently simulate a π^o. In short we would like to be able to "erase" the charged hadron hits.

Figures 5 and 6 indicate the γ-π^o and γ-η^o separation capability as a function of the fiducial area in which the triggering photons appears.

Pions and η^o's were generated with $P_\perp > 3$ GeV/c and were required to simulate a photon of $P_\perp > 3$ GeV/c either by the loss of a photon out of an edge of the detector or the inability to separate the showers of the two photons. We assume that we can resolve 2γ from 1γ provided the 2γ physical separation is ≥ 1.5 cm.

VI. Formal Request

At the present time we do not perceive any rigging, electronic or mechanical needs beyond those required for E-515. The matter of additional computing time and liquid nitrogen refrigerant is negotiable.

We request 300 hours of specific running time. We feel that this time should be adequate for getting a variety of diagnostic test data including a good subset for planning an extended high $P_\perp$ single photon inclusive study and a good 100-200 hour block of high mass multiphoton data. The latter should constitute a real and competitive $\eta_c \rightarrow \gamma\gamma$ experiment.

This work requires less demanding beam optics, beam intensity and fewer spectrometer subsystems than E-515. We feel that this experiment is consonant with the developement of the E-515 program.

Figure Captions

Figure 1 - Plan view of the E-515 apparatus.

Figure 2 - Elevation view of the E-515 apparatus.

Figure 3 - Art work for the vertical readout strips of the liquid argon detector

Figure 4- Artwork for the horizontal readout strips showing the placement of the auxillary Pb - glass wall.

Figure 5-The fraction of π^o's which simulate photons at $P_\perp > 3$ GeV/c as a function of fiducial area for the trigger photon.

Figure 6- The fraction of η^o's which simulate photons at $P_\perp > 3$ GeV/c.

References

1. Copious Direct Photon Production: A Possible Resolution of the Prompt Lepton Puzzle. G. Farrar and S. Frautschi, PRL 36 (1976)1017.

2. Experimental Means For Distinguishing Models of Large $p_\perp$ Inclusive Scattering, G. Farrar, Phys. Lett. 67B (1977) 337.

3. Measuring QCD Compton Effects, H. Fritzsch and P. Minkowski, Phys. Lett. 69B(1977) 316.

4. Testing Quantum Chromodynamics in the Hadroproduction of Real and Virtual Photons, F. Halzen and D. M. Scott, PRL 40 (1978) 1117.

5. Production of Real Photons at Large Transverse Momentum in PP Collisions, R. Riichl et. al., SLAC Pub. 2115, May 1978.

6. Large Transverse Momentum Photons From High-Energy Proton-Proton Collisions, P. Darriulat et. al., Nuclear Phys. B110(1976) 365-379.

7. Search For Single Photon Direct Production in $p^{+}p$ Collisions at $\sqrt{s}$ = 53 GeV., E. Amaldi et. al., Physics Lett. 77B(1978)240.

8. Observation of a Meson $X \rightarrow 2\gamma$ With Mass 2.85 GeV/c^2 Produced in the Charge-Exchange Reaction $\pi^{-}p \rightarrow Xn$ at 40 GeV/c, W. D. Apel et. al., Phys. Lett. 72B(1978) 500.

9. Production of Hadrons at Large Transverse Momentum at 200, 300, and 400 GeV, J.W. Cronin et. al., Phys. Rev. D 11 (1975) 3105.

10. Measurement of the Dihadron Mass Continuum in P-Be Collisions and a Search for Narrow Resonances, R. D. Kephart et. al., PRL 39(1977) 1440.

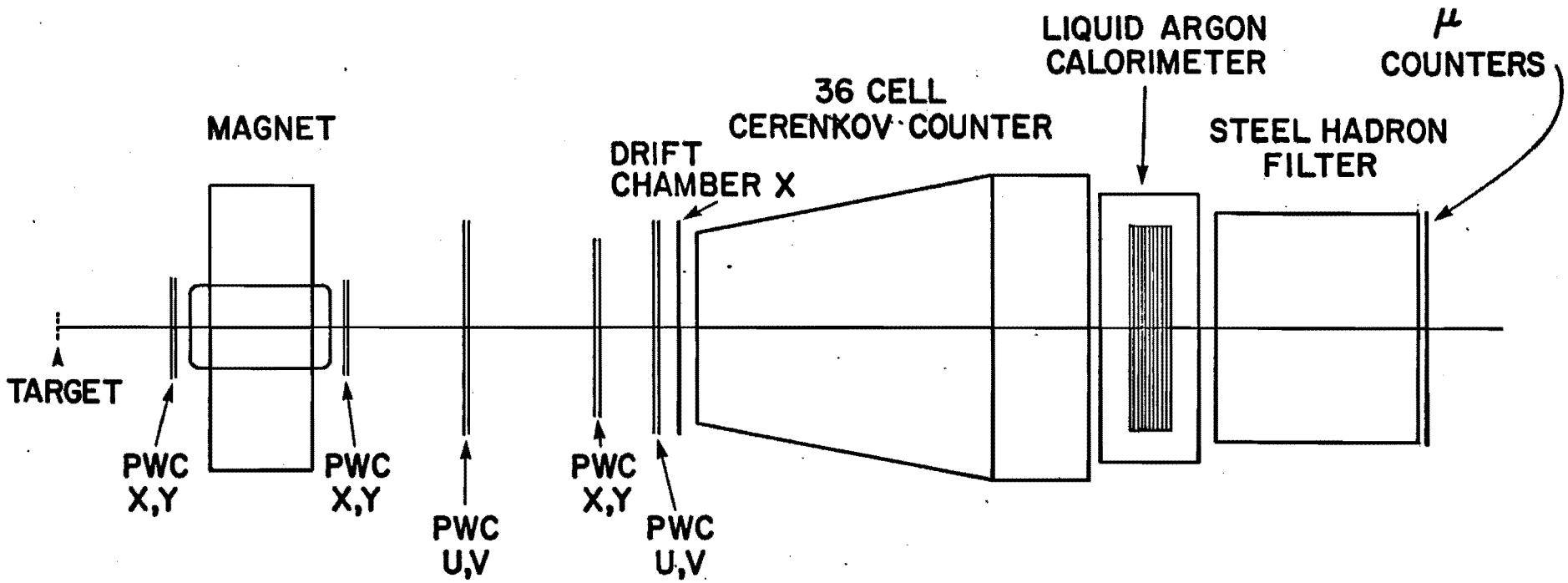

E515 PLAN VIEW

Figure 1

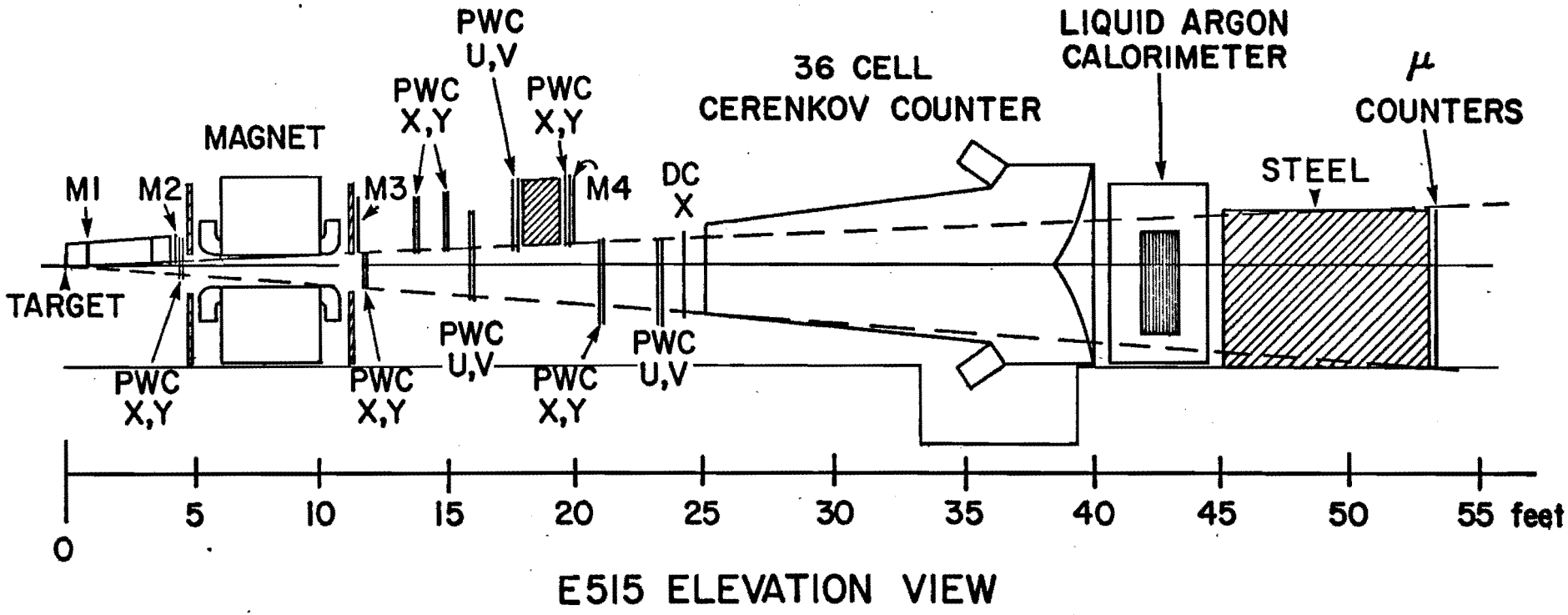

E515 ELEVATION VIEW

Figure 2

Figure 3

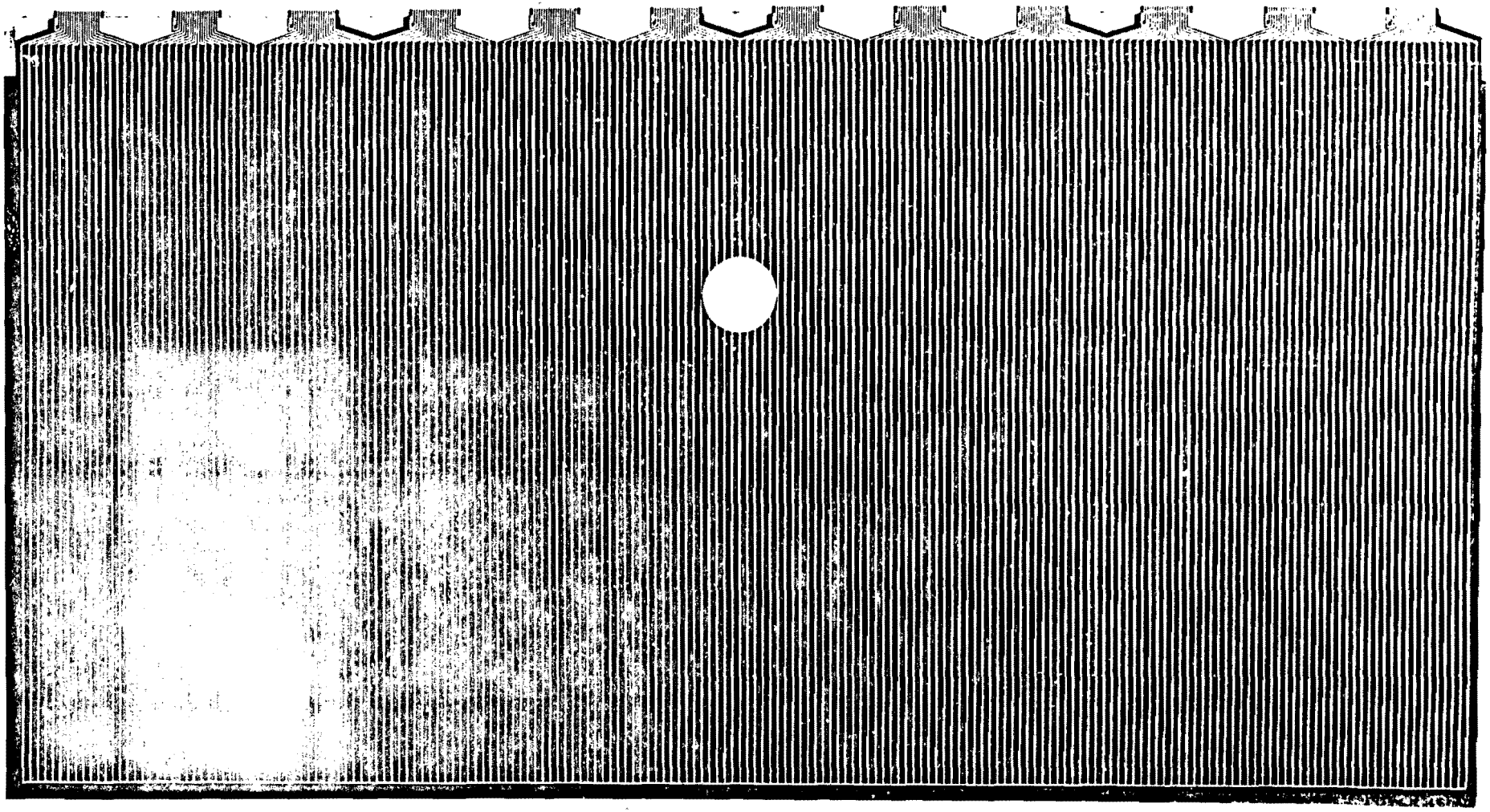

Figure 4

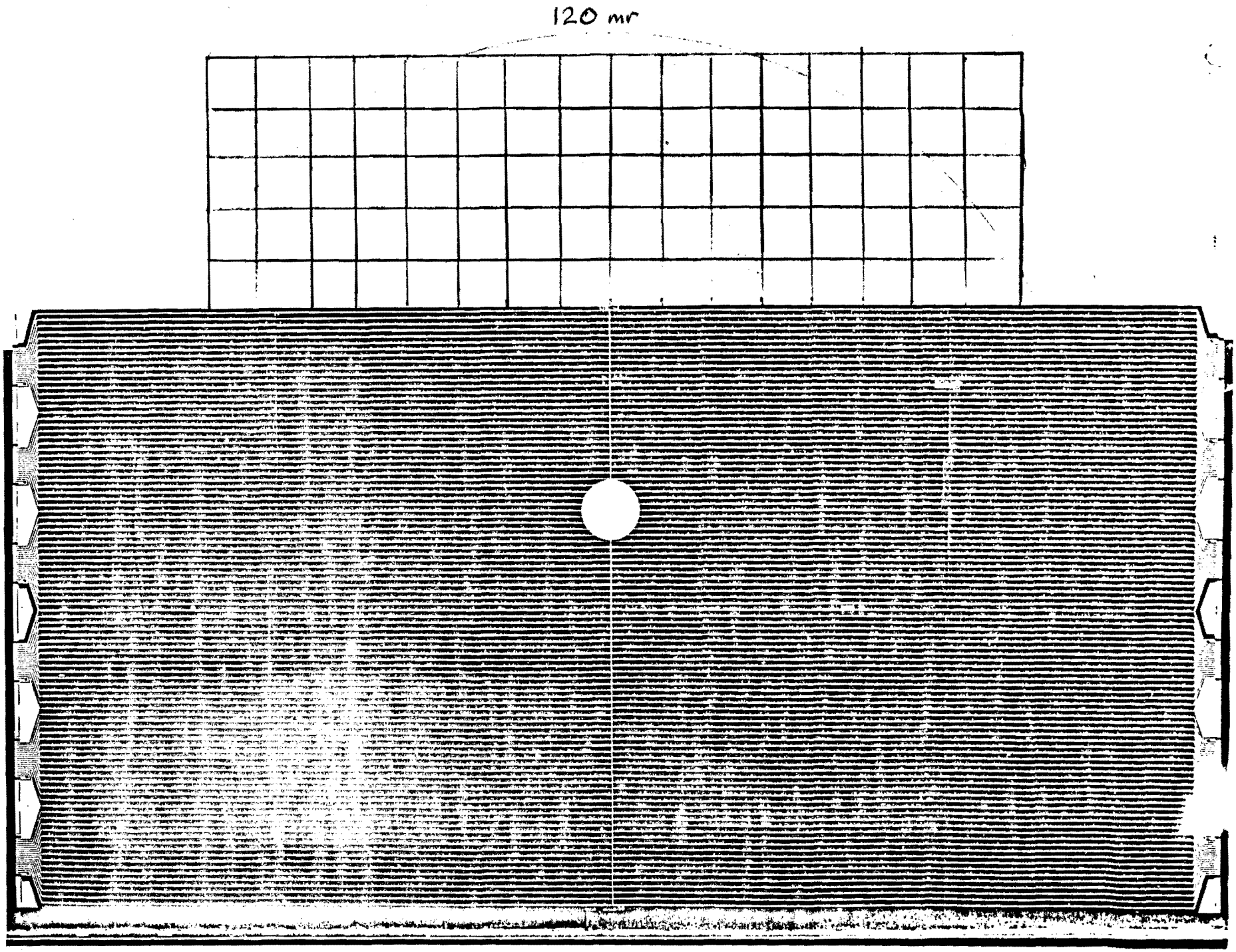

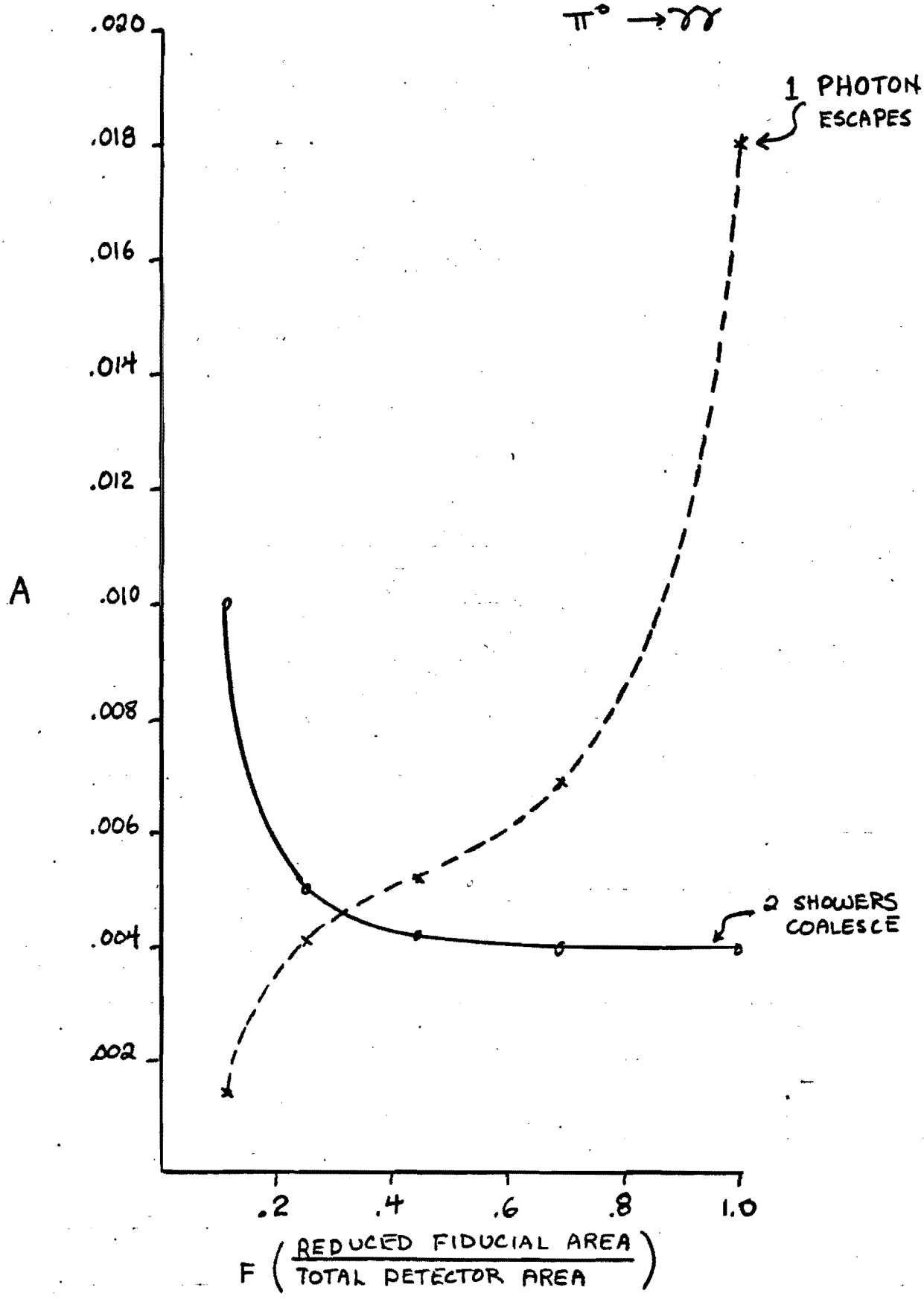
$A \equiv \frac{\pi^0 \to \gamma\gamma \text{ (SIMULATES SINGLE } \gamma)}{\pi^0 \to \gamma\gamma \text{ BOTH } \gamma\text{'S DETECTED}}$
$\pi^0 \to \gamma\gamma$
1 PHOTON ESCAPES
2 SHOWERS COALESCE
A
.020
.018
.016
.014
.012
.010
.008
.006
.004
.002
.2
.4
.6
.8
1.0
F (REDUCED FIDUCIAL AREA / TOTAL DETECTOR AREA)

Figure 5

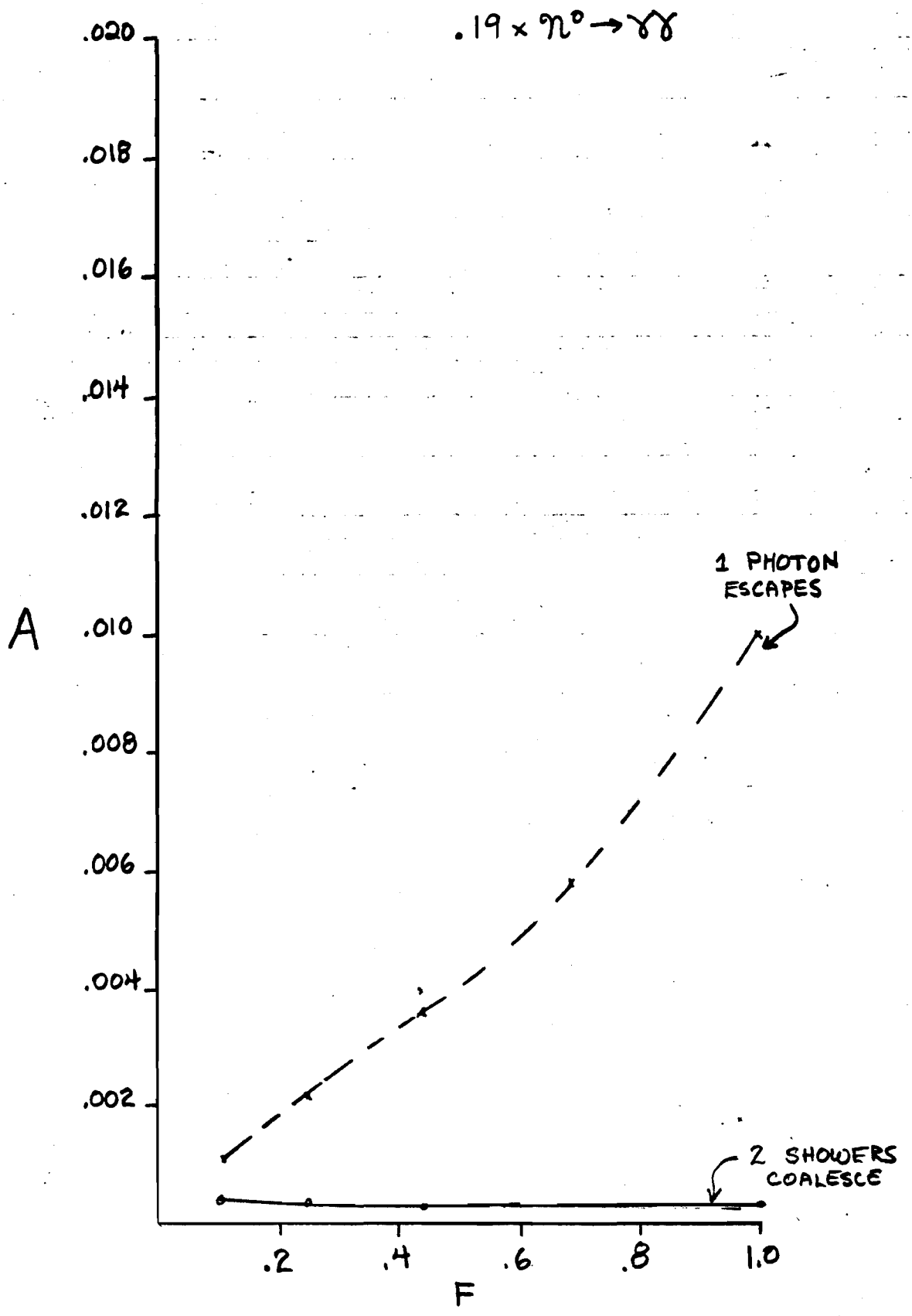
.19 × η° → γγ
.020
.018
.016
.014
.012
.010
.008
.006
.004
.002
A
1 PHOTON ESCAPES
2 SHOWERS COALESCE
.2
.4
.6
.8
1.0
F

Figure 6

NAL PROPOSAL NO. 614
ADDENDUM

Scientific Spokesman:

J. Rosen
Northwestern University
Department of Physics
and Astronomy
Evanston, Illinois 60201

Comm: 312-492-5457

STUDY OF HIGH MASS MULTIPHOTON STATES AND DIRECT PHOTON PRODUCTION

Northwestern University

Notre Dame University

Carnegie Mellon University

Fermilab

Rutgers University

April, 1981

ADDENDUM TO P614

ADDENDUM TO P614

I. INTRODUCTION

P614 was originally proposed in early 1979. It was proposed to use the 2.8 m^2 finely sectorized liquid argon shower calorimeter built for E515 to initiate a study of direct photon physics. It was argued that a preliminary direct photon study was possible with E515 preparations. This was based on the fact that the E515 spectrometer system would come into operation after the shower detector was ready. Nevertheless, the proposal was deferred.

In the fall of 1980 we requested reconsideration of P614. We proposed to initiate the construction of an improved second generation shower detector. Since that time the accelerator schedule was revised to include a fall, 1981 run. In order to meet this schedule we have chosen an intermediate course. We propose to run E614 with modified internal segmentation in the present liquid argon detector. This will allow us to analyze multi-photon events with improved reconstruction efficiency. The improved detector will remain in its present position in the E515 spectrometer and is compatible with E515 operation. In terms of acceptance this configuration is similar to the original P614 arrangement.

II. PHYSICS GOALS

The physics goals of the revised P614 are substantially the same as those of the initial proposal. Briefly stated, they are:

A. Measure the production of photons at large transverse momentum.

B. Measure the hadronic state associated with large P_t direct photons.

C. Measure the production at large transverse momentum of low mass resonances (π^0, η^0, $\eta^{0\prime}$, ω, ...) which decay into photons.

D. Search for high mass states which decay into photons or electrons (η_c, η_b, $\Upsilon \to 2e$, ...) up to masses of 10 GeV.

E. Search for a high mass diphoton continuum.

F. Search for high mass states which decay into charged particles. A high mass multi-photon trigger or a high P_t multi-photon trigger will select events where "hard" collisions have occurred. We can then examine these events for heavy quark production and high mass resonant states.

We would like to comment on the position of our experiment vis-a-vis published ISR results. Due to the larger center of mass energy at the ISR, these experiments have access to a larger range of photon transverse momentum. However:

1. Our acceptance and luminocity are larger.
2. Our ability to separate photons from π^0's on an event-by-event basis is better. This is due to our improved acceptance and the fact that our photons are an order of magnitude more energetic. (The background subtraction in the best ISR results is comparable to the magnitude of the signal.)
3. We can study high mass multi-photon systems.
4. We can target pions as well as protons (this is dependent on planned Meson Lab construction).

The second point is especially important when we study the hadronic state associated with candidate single photons.

III. IDEALIZED EXPERIMENT

We first consider an idealized experiment with a realistic, optimized shower detector. In Section IV we will discuss the the extent of the compromises that will result from the use of the modified E515 shower detector.

Visualize a flat, finely sectorized shower detector with circular boundaries corresponding to polar angle bounds, θ_1(inner) and θ_2(outer). There is full coverage in azimuth angle (ϕ), and within the specified boundaries there are to be no dead regions. Figure 1(a) illustrates the detector coverage in the $x_\perp$, $x_\parallel$ plane. We choose the acceptance wedge to correspond to $\theta_1 = 45^o$ and $\theta_2 = 120^o$. This corresponds to 60 percent of the CM total solid angle (71 percent of the forward hemisphere and 50 percent of the backward hemisphere).

Figure 1(b) shows this region Lorentz transformed into the laboratory. It is readily seen that extending the detector coverage beyond $\theta_2 = 120^o$ (θ_2(LAB) = 1.73 γ_{cm}^{-1}) is not very cost effective. The periphery of the detector grows rapidly for an increasingly marginal gain of acceptance in the backward hemisphere. It is generally well known that the transformation Jacobean is a rapidly shrinking function of θ.

In fact, if θ is reduced from 120^o to 90^o, excluding negative x, the detector area will be reduced by more than a

factor of 3 and the acceptance will drop from 60 percent to 35 percent.

The accepted range of x is largest at large $x_\perp$, which is the interesting regime, and smallest at the value of $x_\perp$ which is characteristic of the bulk of the particle production ($P_\perp \gtrsim$ 0.5 GeV/c). Hence the average hadron multiplicity per interaction in the shower detector will be more than an order of magnitude smaller than the total multiplicity.

The basic readout will be x-y strips arranged in quadrants. We believe that this is optimum for a number of reasons:

A. All the strips terminate on the outer boundary and the readout can be effected without difficulty or dead regions.
B. The strip widths are uniform and the projected shower shape is position invariant. Tapering strip widths, which would characterize r,θ systems or spiral systems, could be a pattern recognition nuisance.

If the superiority of the x-y readout system is conceded, it is natural then to reconfigure the outer boundary into a square, keeping the detector area about the same. Figure 2 illustrates the detector geometry as seen from the target.

Interior Detector

Both Figures 1 and 2 show a second interior region bounded by θ_1 and θ_3. We propose to outfit this area with shower detection. This interior detector subtends three-fourths of the area of the forward hole. The readout will be from the θ_3 surface. The alternating u-v coordinates are illustrated in Figure 3. We plan 120 coordinates of each. Clearly, the strips increase in width as a function of radius. Nevertheless, the pattern recognition task will be facilitated by the fact that each strip (u or v) intersects only 14 percent of its opposite number (v or u), i.e., the pattern recognition involves only 14 percent of the azimuthal range.

This interior detector will not be part of the trigger but will be of utility. The efficiency of γ detection will be improved, consequently neutral hadron detection efficiency will accrue for π°, η°, ... This will improve the hadron rejection in the direct γ channel.

The boundary region between the main detector and the interior detector will be virtually seamless--an important virtue of the liquid argon ionization detector.

Ideal Detector (Continued)

Our choice for the appropriate dimensions for a new detector would be 3 m x 3 m, cell widths 1 cm. In order to maintain the sharpest possible shower profiles, the readout art work (P.C. boards) would vary (slightly) with detector depth. The shower cells would, in effect, "focus" on target. This is an important consideration at the largest intercepted angles (0.15 radians).

IV. DESCRIPTION OF THE P614 LIQUID ARGON SHOWER DETECTOR

A. Overall Description

The detector consists of a matrix of lead sheets and etched printed circuit boards. The matrix contains 28 longitudinal cells, each with a 3 mm lead sheet and x-y readout planes. The present lead sheets will be retained.

B. Exterior Detector

The exterior detector will consist of the same x-y boards used in the present detector. These boards will be modified to provide an internal hole 60 cm in diameter into which the inner detector will be inserted. The parameters of the exterior detector are:

Inner diameter	0.6 m
Outer diameter	± 1.2 m (horizontally) + 0.3 m - 0.6 m (vertically)
Cell size	1.25 cm x 1.2 m
Structure	2 halves (front and back) 14 samplings (x and y) in each half

C. Interior Detector

The inner detector (Figure 5) will consist of a set of semicircular P.C. boards attached to the boards of the exterior detector. This system will be essentially as described in Section II. The parameters are:

Inner diameter	0.3 m
Outer diameter	0.6 m
Cell size	0.16 m length 0.0075 m - width - 0.018 m
Number of cells	120 u 120 v

There is no segmentation in depth

This detector is compromised with respect to the idealized detector described in Section III in three ways:

1. The acceptance of the system is reduced.

   In any direct photon experiment fiducial cuts must be made to insure good π^0-γ separation. This amplifies edge effects in the detector. The angular coverage of the improved E515 detector is a factor of 1.5 smaller than that of the idealized detector.

2. The strips are not focused on the target.

   At large angles the spread of the shower due to its angle with respect to the detection cells becomes larger than the intrinsic shower spread $\langle\theta\rangle$. This results in more difficult reconstruction and somewhat reduced resolution in both position and energy. For the angles relevant to the present proposal, we expect the effect to be non-negligible only at the far edges.

3. The segmentation is coarser.

   The P614 detector x-y section will be read out in two halves. The idealized detector has quadrant readout. This results in a factor of 2 decrease in pattern recognition ambiguity.

V. HADRON REJECTION

The primary task for the isolation of direct γ's is the identification of $\pi^\circ, \eta^\circ \to 2\gamma$. (A rather minor problem, which we note in passing, is the interaction of n, $\bar{n}$ and K_L^o in the shower calorimeter. The probability that a neutral hadron will surrender a substantial fraction of its energy in the calorimeter is rather small. Consequently, the apparent P_t of the false shower will be systematically lower than the true hadron P_t. Our extensive experience with e^*-hadron separation indicates that the neutral hadron background will be a minor consideration.)

A powerful direct γ experiment should be characterized by a $\pi^\circ, \eta^\circ \to 2\gamma$ detection efficiency $\geq$ 95 percent, i.e., given a recorded γ with large P_t, the efficiency for detecting the <u>second</u> γ from the $\pi^\circ(\eta^\circ)$ should exceed 95 percent. There are two ways to lose the second γ.

(i.) Second γ missing:

The second γ may either miss the active detector region <u>or</u> have so little energy that the deposited shower ionization charge falls below threshold for effective registration. Note that this is really a correlation problem, since the $\gamma\gamma$ opening angle equals $m_\pi (E_1 E_2)^{-\frac{1}{2}}$.

Figure 1(a) has superimposed on the acceptance region a set of lines corresponding to the fraction of the incident energy that materialized in the γ (or π°, η°). It is easily seen that for E_0 = 400 GeV the energy range of interest is $\sim$(50-150)

GeV. Then $\langle E \rangle \approx 80$ GeV. Using a conservative threshold for γ detection of 1 GeV, the probability that a γ energy will fall below 1 GeV threshold is

$$2\ (1\ \text{GeV})/80\ \text{GeV} = 2.5\%$$

The geometrical probability that the second γ with energy $\geq$1 GeV will miss the detector is less than this percentage if the rim of the detector is excluded from the fiducial area. All of this is confirmed by Monte Carlo simulation.

One can hope to have an effective threshold lower than 1 GeV (perhaps 0.5 GeV), but it is not essential. The danger of including second γ candidates with marginal measurement lies in the fact that the 2γ invariant mass resolution could be very poor and one may reject good direct γ's.

ii. Coalescing $\gamma+\gamma$

When the $\gamma\gamma$ opening angle is very small, the γ's may coalesce. The electromagnetic shower of a single γ has finite transverse extent. In our present detector the strip widths of 1.25 mm exceed the intrinsic shower radius. In the first half of the detector a single shower is largely contained in two strips. Each strip subtends an angle of 0.9×10^{-4} radians. We anticipate a possible difficulty in resolving $\pi^{\circ} \rightarrow 2\gamma$ when the opening angle is less than 2×10^{-4} radians, corresponding to a γ energy of 150 GeV.

The question of π^0-γ separation at the highest energies deserves some comment. The "mass" of a multi-photon system can be expressed as:

$$m^2 = (\sum_{\gamma} E_i)(\sum_{\gamma} E_i(a_i^2+b_i^2)) - (\sum_{\gamma} E_i a_i)_x^2 - (\sum_{\gamma} E_i b_i)_y^2$$

where the a_i, b_i are the x,y photon direction cosines. If we write the sum over photons as a sum over strips in the detector, the spread of the photon showers will introduce an additional effective mass. This additional mass can be written as:

$$M_{\text{single}\,\gamma} = E_\gamma \langle\theta\rangle$$

and adds in quadrature to the multi-photon mass. $\langle\theta\rangle$ is an angle characteristic of the spread of the electromagnetic shower. This was measured in E515 to be 0.7 milliradians. If we assume that the π^0-γ separation is effective up to single $M_{\text{single}\,\gamma}$ of $\sim$100 MeV, we can expect γ identification up to E_γ of $\sim$150 GeV.

From the above discussion, it is evident that clean π^0-γ separation will not be achieved if there is substantial overlap between photons in a single view. This is why the interior detector, which intercepts the bulk of the low P_t photon production, is important. The exterior x-y detector, where the high P_t photons will register, will be relatively free of unrelated hits, simplifying π^0-γ separation at large energies.

VI. PERFORMANCE OF THE E515 LIQUID ARGON DETECTOR

The liquid argon detector built for E515 has proven to be both powerful and reliable. In our previous run, there was no down time registered due to problems with the detector or its associated readout. The energy and position resolution of the detector was calibrated using data taken with low momentum beams (20, 30, 40 GeV). These beams contain a substantial fraction of electrons. The energy and position resolutions for these electrons are demonstrated in Figures 6 and 8.

The shower reconstruction program is now fully operational. In typical E515 data we reconstruct approximately six showers per event with $E_\gamma > 1$ GeV. A typical diphoton mass plot for a single E515 run is shown in Figure 7.

At the end of the spring, 1980 run a test was performed by adding a 1% concentration of methane to the argon in the detector. This resulted in a factor of 2 decrease in the charge collection time and a 30 percent loss in pulse height. We are currently operating the detector in this mode.

VII. ACCEPTANCE AND RESOLUTION

Figure 1(a) summarizes the single photon acceptance (at 400 GeV) of the proposed detector. The geometric acceptance is given by the solid lines θ_1, θ_2 and θ_3. These represent limits imposed by the inner edge of the x-y section, the outer edge of the x-y section, and the inner edge of the u-v section, respectively. The shaded region represents the kinematic regime where single photon measurements will be made. This region is defined at low $x_\perp$ by the P_t trigger threshold of roughly 3.5 GeV/c. At high $x_\perp$ low statistics prevail. In the high x and $x_\perp$ region, π° coalescence is the limit.

In the region where direct photons will be measured, the resolution in P_t is determined by the shower energy resolution:

$$\sigma(E) \cong 0.18/E^{\frac{1}{2}}$$

so

$$\delta P_t/P_t \cong 0.18/E^{3/2}$$

A related question is the relative calibration of the π° and single photon spectra. Because we are taking the ratio of two rapidly falling distributions, any error in the scale of either will result in a large error in the ratio. This can be addressed by deliberately choosing <u>asymmetrical</u> π° decays. The P_t of of these π°'s will be dominated by the high energy photon, which can then be compared directly to single γ's of the same P_t.

The hadronic state will be measured by the E515 charged particle spectrometer. The geometrical acceptance of the spectrometer is indicated in Figure 3. The current reconstruction program finds an average of 6 charged tracks/event. The track finding efficiency is > 95 percent for the complicated multiparticle states we see in association with the μ trigger. We anticipate having an imaging cerenkov counter installed for testing during the 614 run. If this works as expected, we will be able to measure quantum numbers within the away-side jets.

How well one measures an object as poorly defined as a jet is a difficult question to answer. Our single particle acceptance extends into the backward hemisphere. The asymmetric acceptance imposed by the E515 geometry will reduce our acceptance slightly. The acceptance for charged particles emitted at 90^{o} in the center of mass remains greater than 70 percent.

VIII. TRIGGER RATES

Our acceptance and expected trigger rates are similar to those estimated in the original proposal. The numbers are modified slightly due to changes in the fiducial area definitions and a larger target-detector separation. We will summarize the results.

A. High Mass Multi-Photon States

Our acceptance for 2γ states is roughly 40 percent and flat in mass above 3 GeV. Assuming 10^6 interactions/pulse, we expect

1/event/pulse/80nb

In particular, for the decay $\eta_c \longrightarrow 2\gamma$, we expect to be sensitive to a cross section

$$\sigma(p + Be \longrightarrow \eta_c + X) \geq 2 \text{ nb.}$$
$$\qquad\qquad\qquad\quad \hookrightarrow 2\gamma$$

B. High P_t Direct Photon Production

In this mode, the acceptance is approximately 65 percent and almost independent of P_t. We expect: 1 event/pulse/50nb. We estimate our yield of events using the measured charged pion production cross section and assuming the γ/π ratio is approximately 0.1 independent of P_t.

The event rates are shown in Table 1.

IX. RUNNING TIME REQUEST AND SCHEDULE

We feel that a 1000 hour run in the fall of 1981 will provide us with adequate statistics to explore the direct photon yield up to a P_t of 7 GeV/c. We will require a positive beam with momentum as close to to 400 GeV/c as is possible in the M1 West line. We note that the proposed detector layout is identical to that of E515. Given the low E515 trigger rate (15/spill), it may be possible to run the μ trigger and a prompt photon trigger simultaneously. As a result of our preliminary trigger studies in the spring of 1980 (Figure 10), we believe a workable photon trigger is already in hand. The mass trigger processor (Appendix I) is already operational.

Our schedule for the rebuilding of the shower detector is shown in Figure 12. We want to emphasize that the detector was designed to come apart easily--there are no solder joints in the interior. All the plumbing and superstructure will be left intact. We view the modifications to the shower detector as an improvement of the E515 spectrometer independent of direct photon considerations.

CONCLUDING REMARKS

It may be noted that we have not included extensive theoretical references. There are no Feynman graphs portraying the now familiar Q.C.D. Compton and annihilation processes. Clearly, it would be interesting to compare different hadronic species, particularly π^+ and π^-, and it would be desirable to extract structure functions. We hope we have made it clear that we have good coverage in $x_\perp$ but relatively limited coverage in $x_\parallel$. This proposal addendum includes less discussion of various event rates than the original submitted two and one-half years ago. The background material which we have either omitted or compressed is amply and redundantly covered in other available proposals.

There are now three newly approved CERN experiments to study direct photon production with secondary hadron beams. There is a similar proposal involving the construction of a new liquid argon shower detector which has been submitted to Fermilab by the Slattery group. All of these experiments involve beam tagging equipment, P.W.C.'s, etc., and consequently are restricted to approximately equal beam flux limitations--10^7 particles/sec and approximately 5 percent interaction length targets. All of the experiments have comparable target-detector separation, energy and position resolution and angular separation. There is surprisingly little variation

in the physics capabilities of the individual efforts. Our present detector has about 50 percent of the geometric acceptance of these as yet unconstructed shower detectors. We can pursue this physics one year earlier.

We would like to particularly emphasize the following point. It is naive to compare the relative merits of the different experiments by comparing the authors' projected event rates. The adopted phenomenologic production models, Monte Carlo codes, efficiencies, etc. may be evaluated differently and with varying degrees of realism and conservatism. Fundamentally, they differ only in the final state geometric efficiency. An experiment which requests 160 days is not better designed than one which requests 60 days!

We would welcome an opportunity for a frank discussion of the relative merits of the different shower detection systems at the time of oral presentation.

TABLE I

YIELD OF MEASURED SINGLE PHOTONS
(PER 1000 HOURS)

P_t >	Events
3	1.2×10^6
4	67 K
5	4 K
6	250
7	15

FIGURE CAPTIONS

1. (a) Single photon acceptance for an ideal detector in the $x_\perp, x_\parallel$ plane. The solid lines indicate the geometrical boundaries. The shaded region indicates where useful measurements of the γ/π^o ratio can be made (θ_1 is the outer detector inner boundary; θ_2 is the outer detector outer boundary; and θ_3 is the inner detector inner boundary).

   (b) The acceptance shown in 1(a) projected into the laboratory frame.

   (c,d) Same as above for P614 detector.

2. Transverse profile of an "Ideal" detector. The angles are as discussed above.

3. Transverse profile of the shower detector (modified for E614) as presently located. The dashed line indicates the boundary of the wire chamber spectrometer acceptance.

4. E515 spectrometer, elevation view.

5. A schematic of the u-v coordinate system for the inner detector.

6. Shower energy deposited by a 18 GeV beam. The energy resolution is approximately 5 percent (sigma).

7. Diphoton mass spectrum from E515 data. Each shower is required to have an energy greater than 4 GeV. The π^o mass resolution is about 14 percent.

8. Position as determined from the shower centroid minus the position found by extrapolating 20 GeV beam tracks to the argon calorimeter. The resolution is consistant with the error in the track extrapolation.

9. The fraction of energy contained in a single (1.25 cm) strip as a function of the distance of that strip from the centroid of the shower. This is for 40 GeV beam electrons (35 events).

10. Trigger rate versus P_t threshold for a simple summed P_t trigger. This data was taken at the end of the spring, 1980 run of E515. The trigger is confined to the x east strips.

11. Monte Carlo results for the ratio of false single photons (coalescing or 1 lost) to reconstructed as a function of P_t. The two curves represent a 5 cm and 7 cm fiducial cut on the outer edge.

12. Schedule for modification of the argon detector.

13. Schematic of mass trigger logic.

FIGURE 1
DIRECT PHOTON ACCEPTANCE (IDEALIZED DETECTOR)

(a) CM

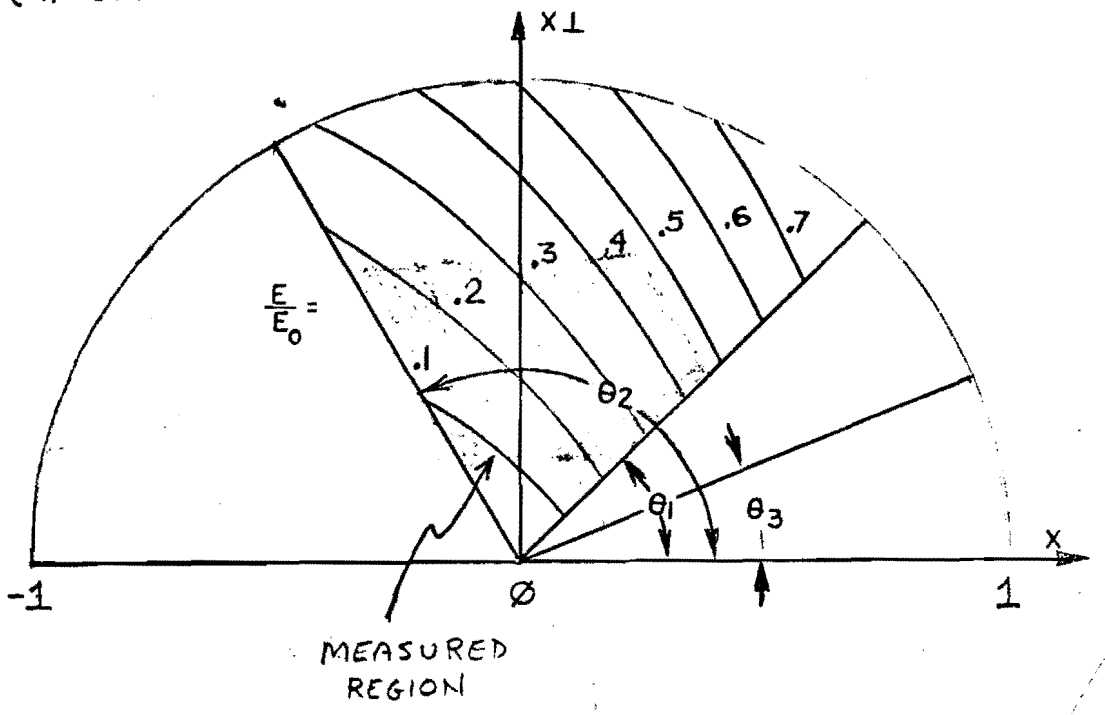

(b) LAB

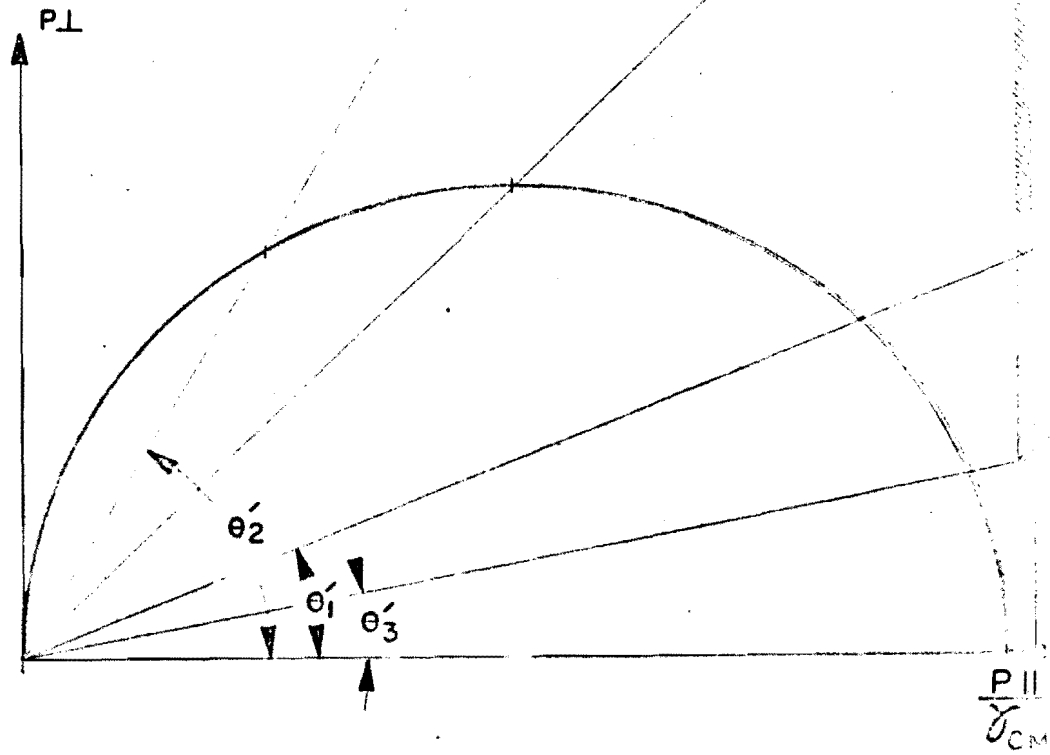

FIGURE 1
DIRECT PHOTON ACCEPTANCE (P-614 Detector)

(c) CM

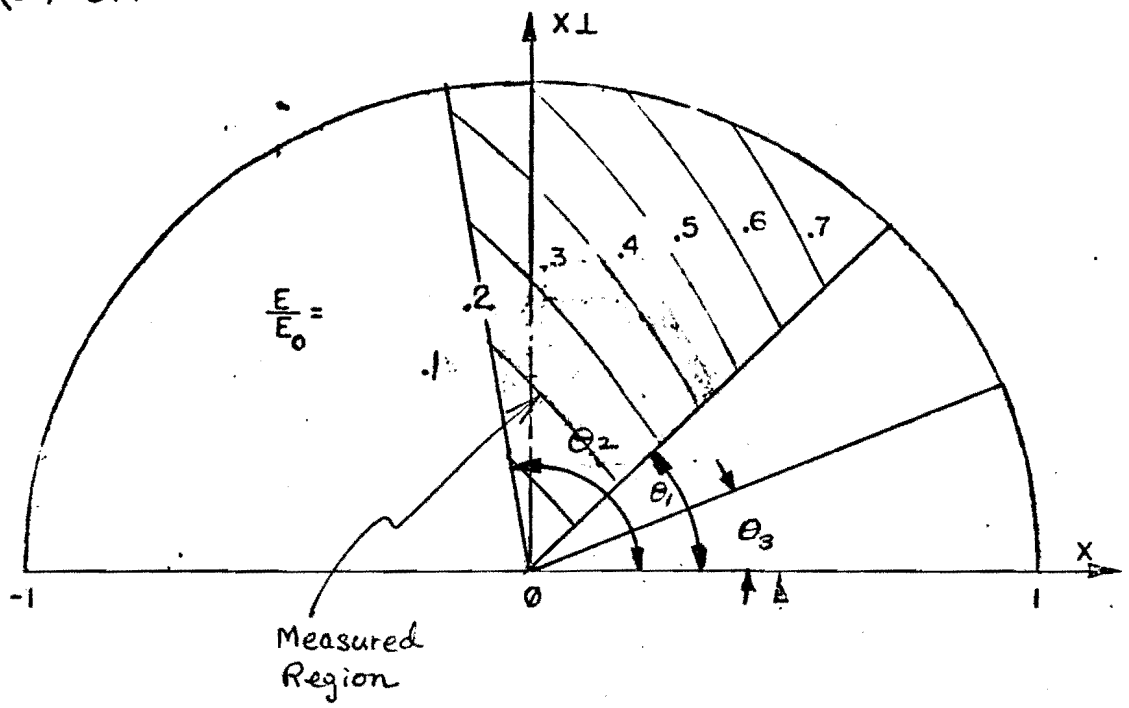

(d) LAB

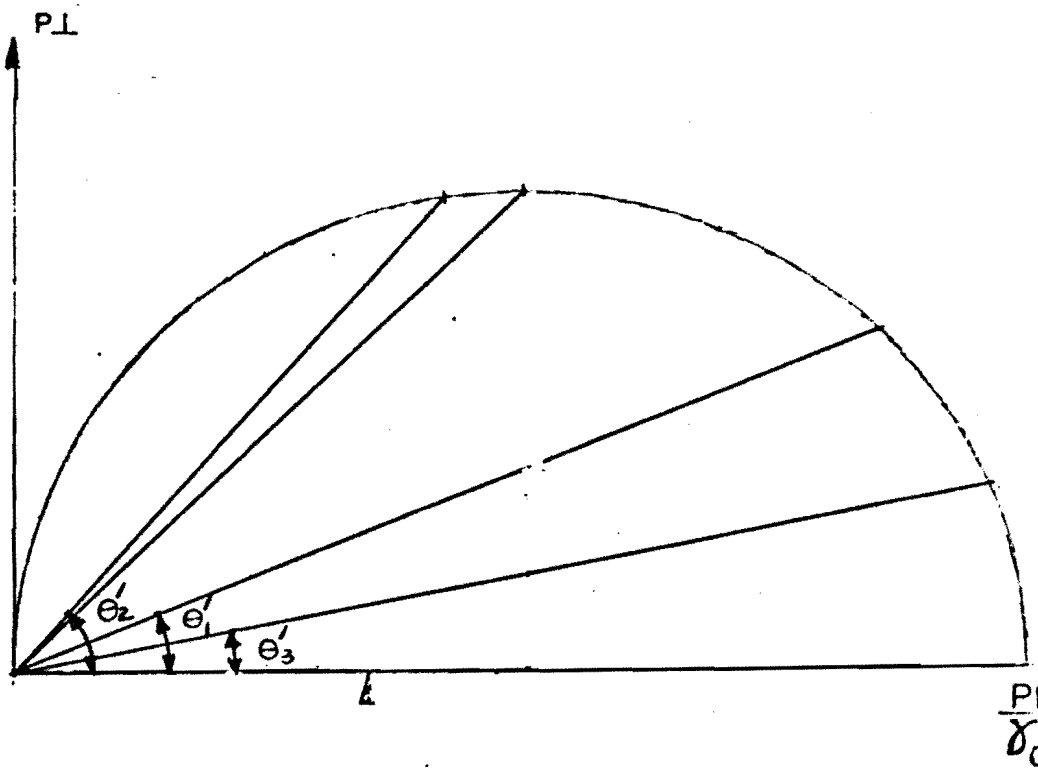

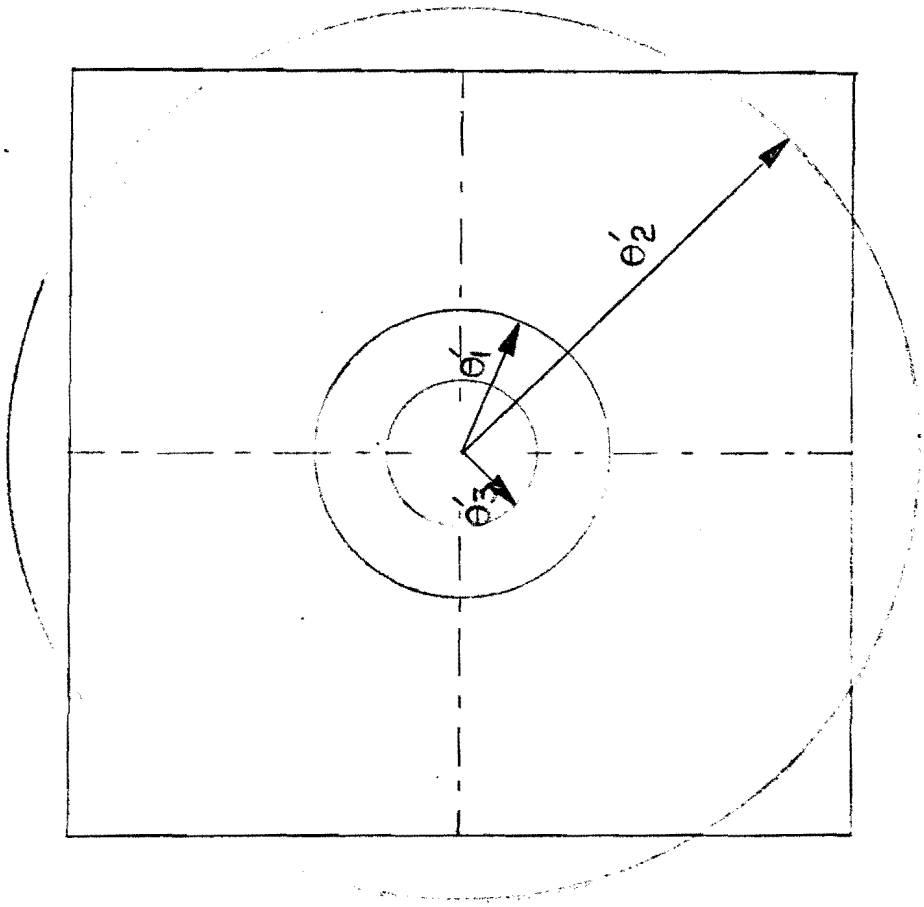

FIGURE 2

PROFILE OF THE "IDEAL" DETECTOR

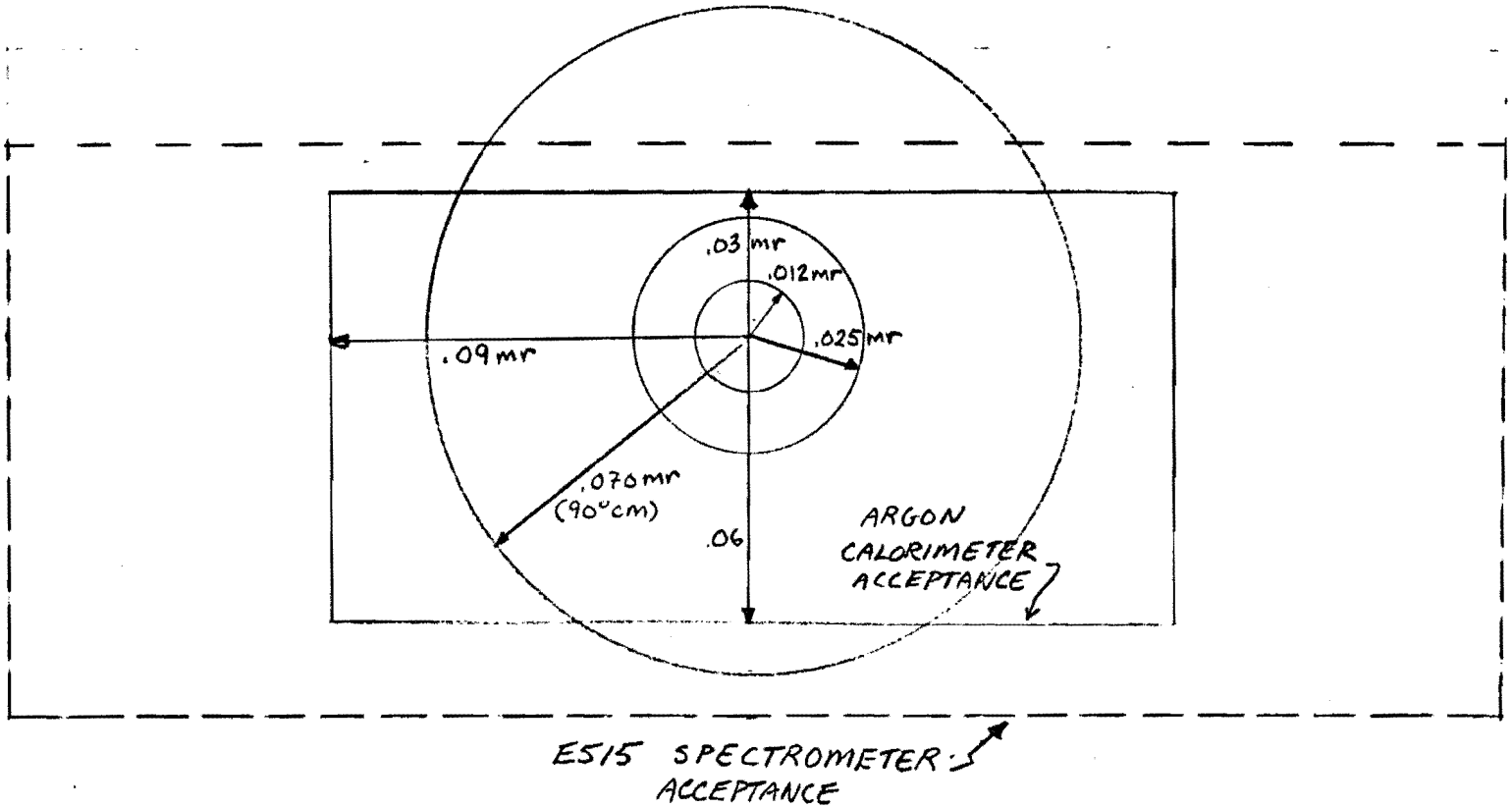

FIGURE 3

ACCEPTANCE OF THE P614 DETECTOR

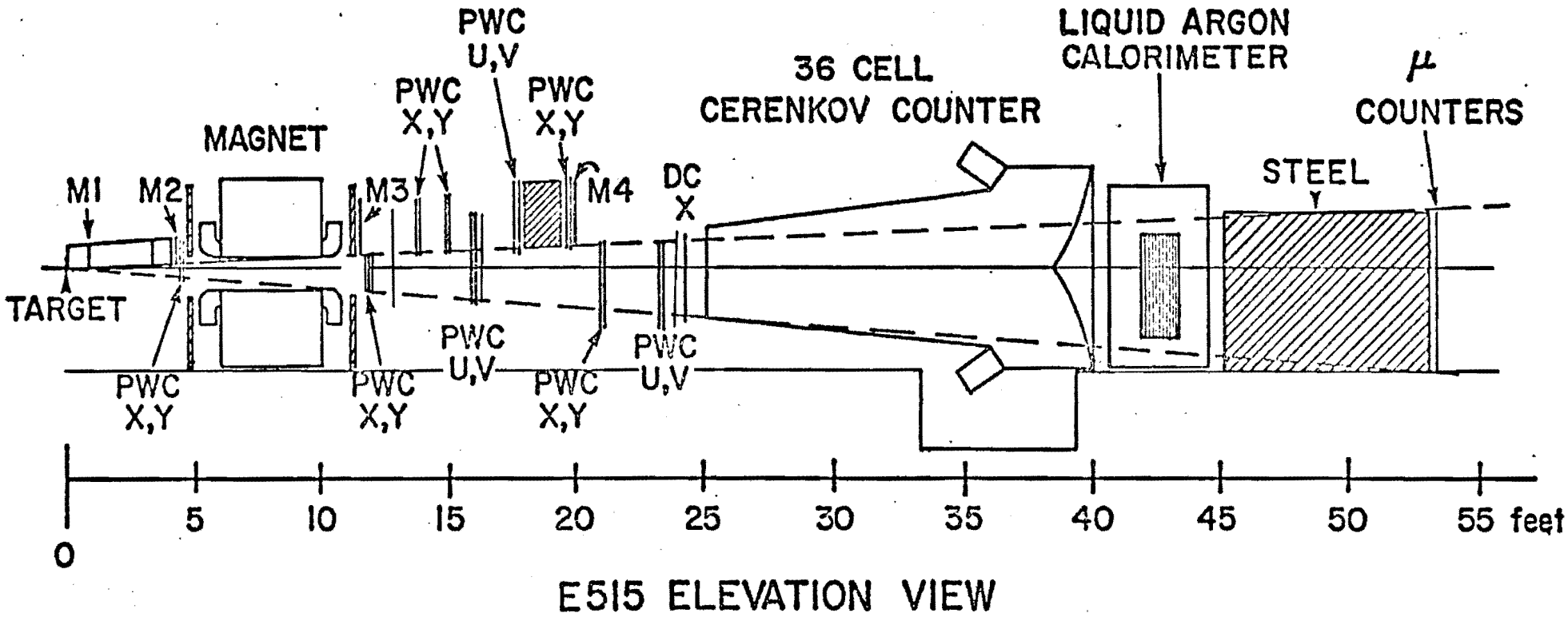

E515 ELEVATION VIEW

FIGURE 4

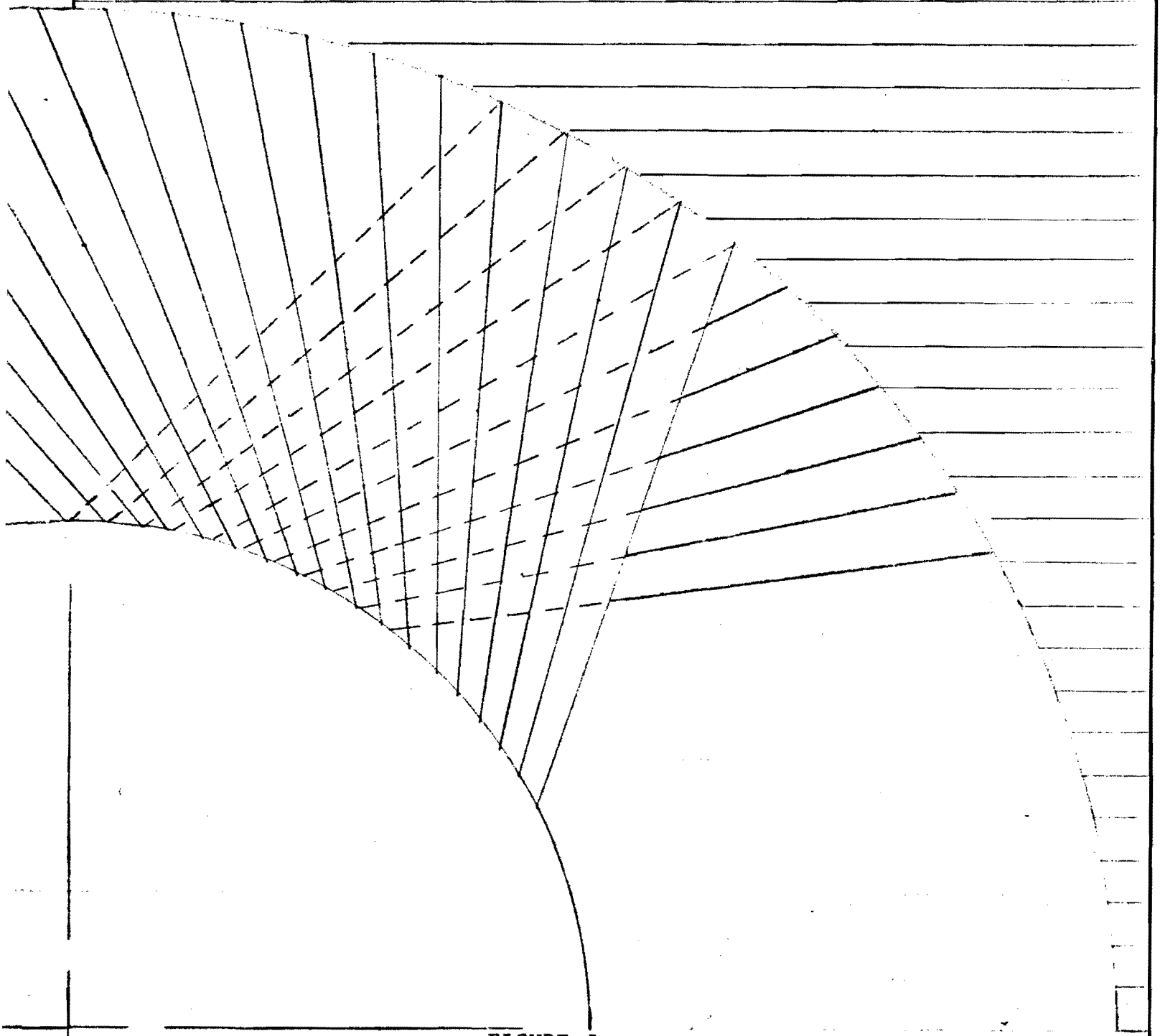

FIGURE 5
SCHEMATIC OF THE INNER DETECTOR

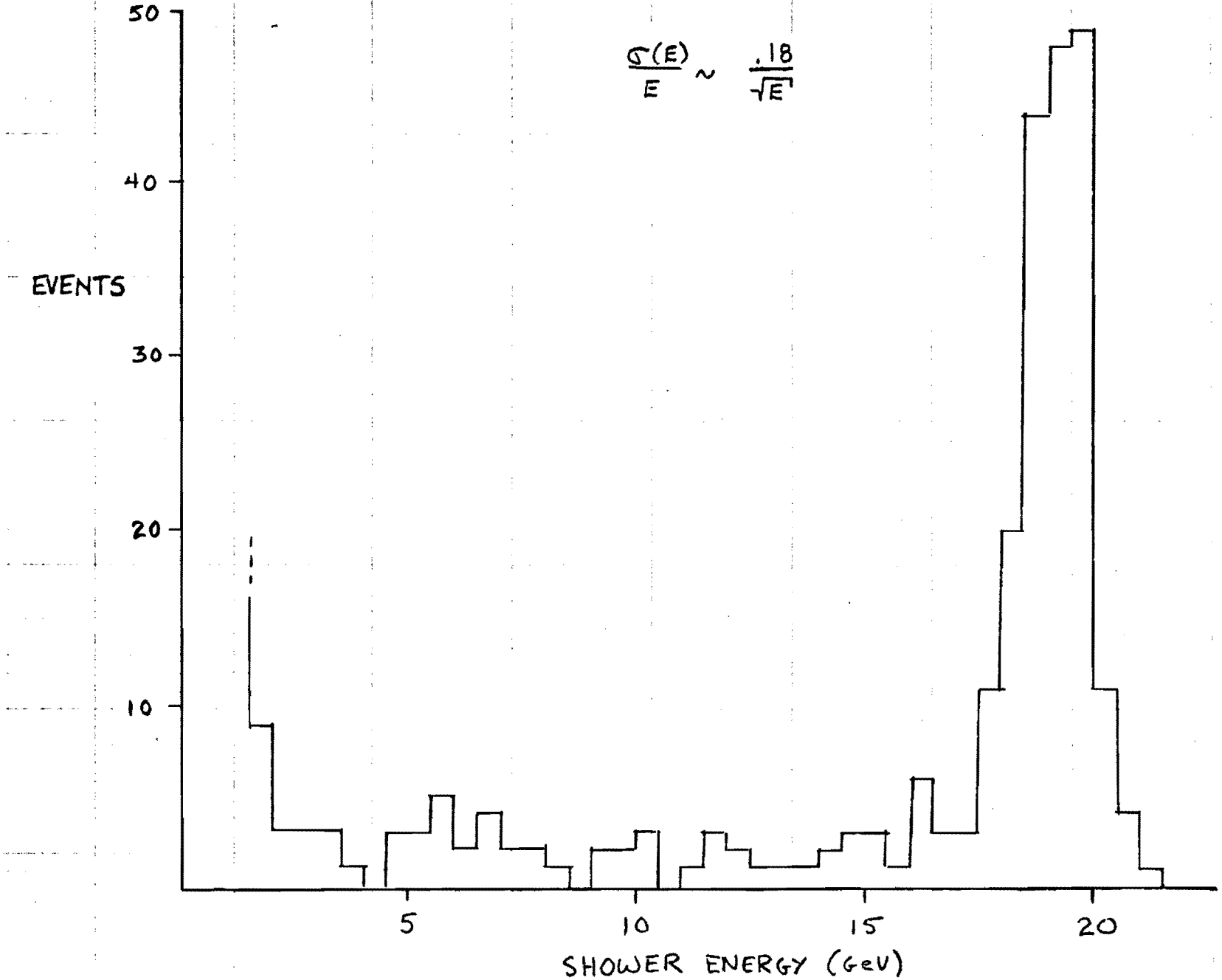

FIGURE 6
18 GeV BEAM SPECTRUM

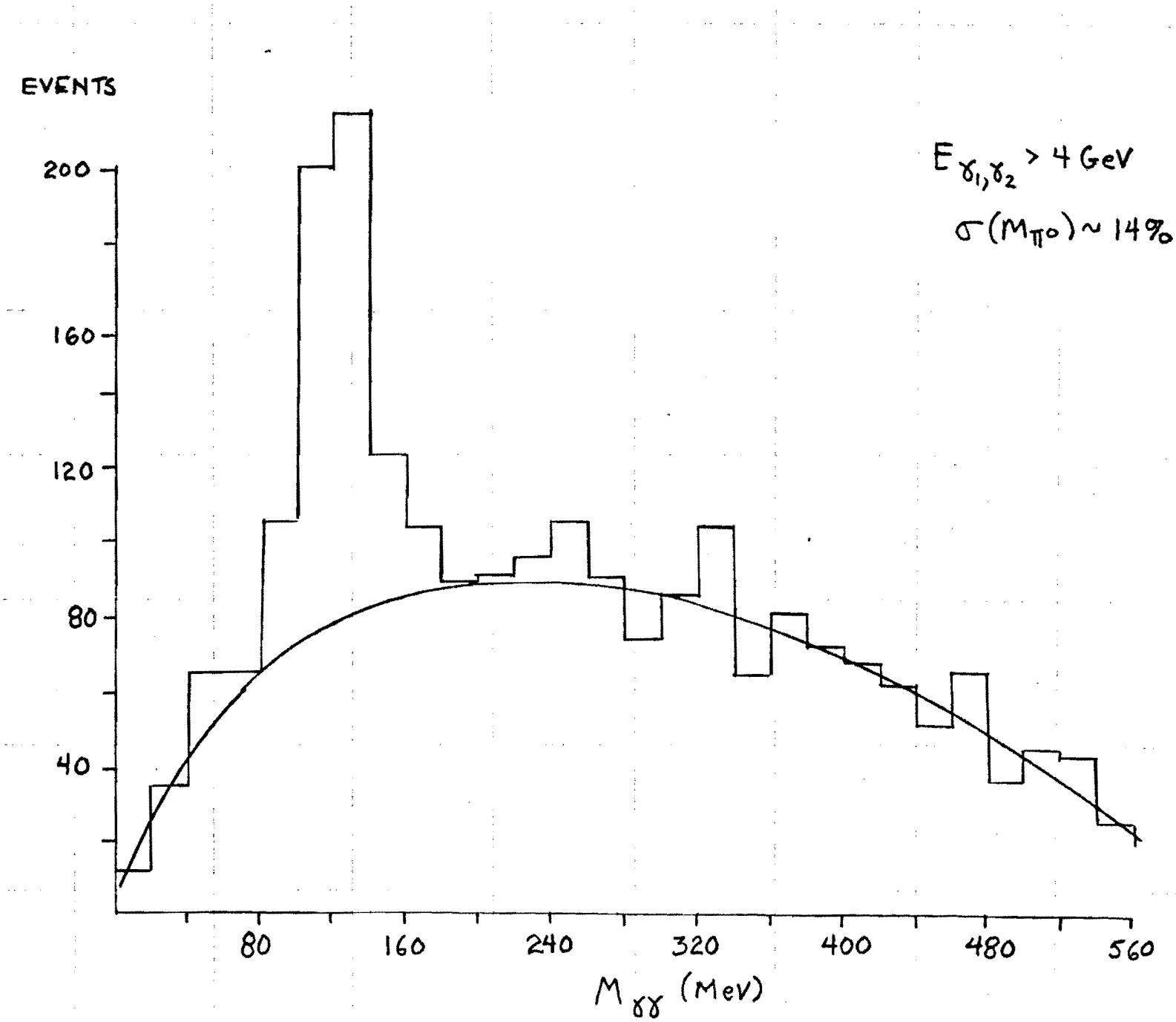
EVENTS
200
160
120
80
40
$E_{\gamma_1,\gamma_2} > 4$ GeV
$\sigma(M_{\pi^0}) \sim 14\%$
80
160
240
320
400
480
560
$M_{\gamma\gamma}$ (MeV)

FIGURE 7

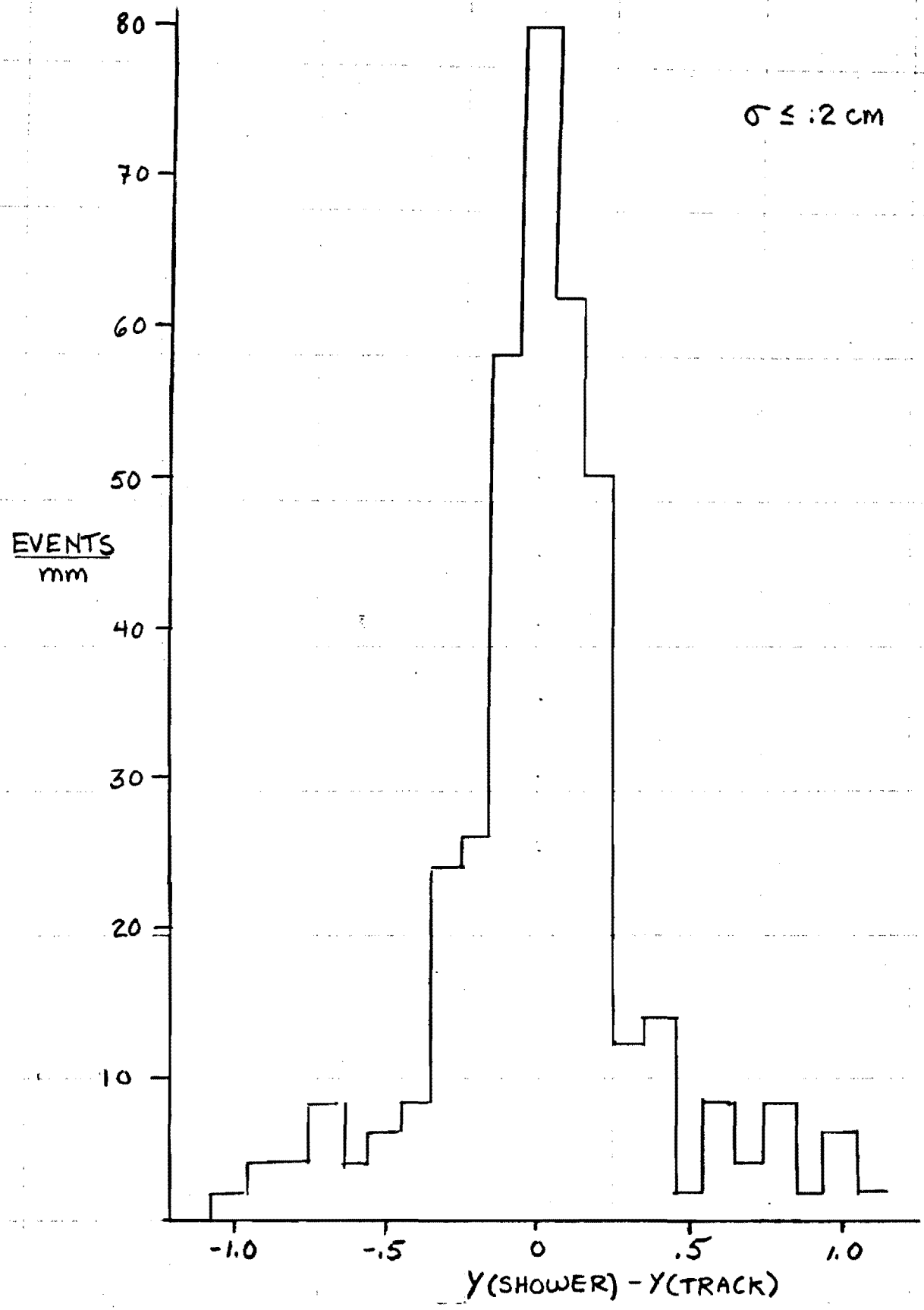

FIGURE 8
LIQUID ARGON POSITRON RESOLUTION

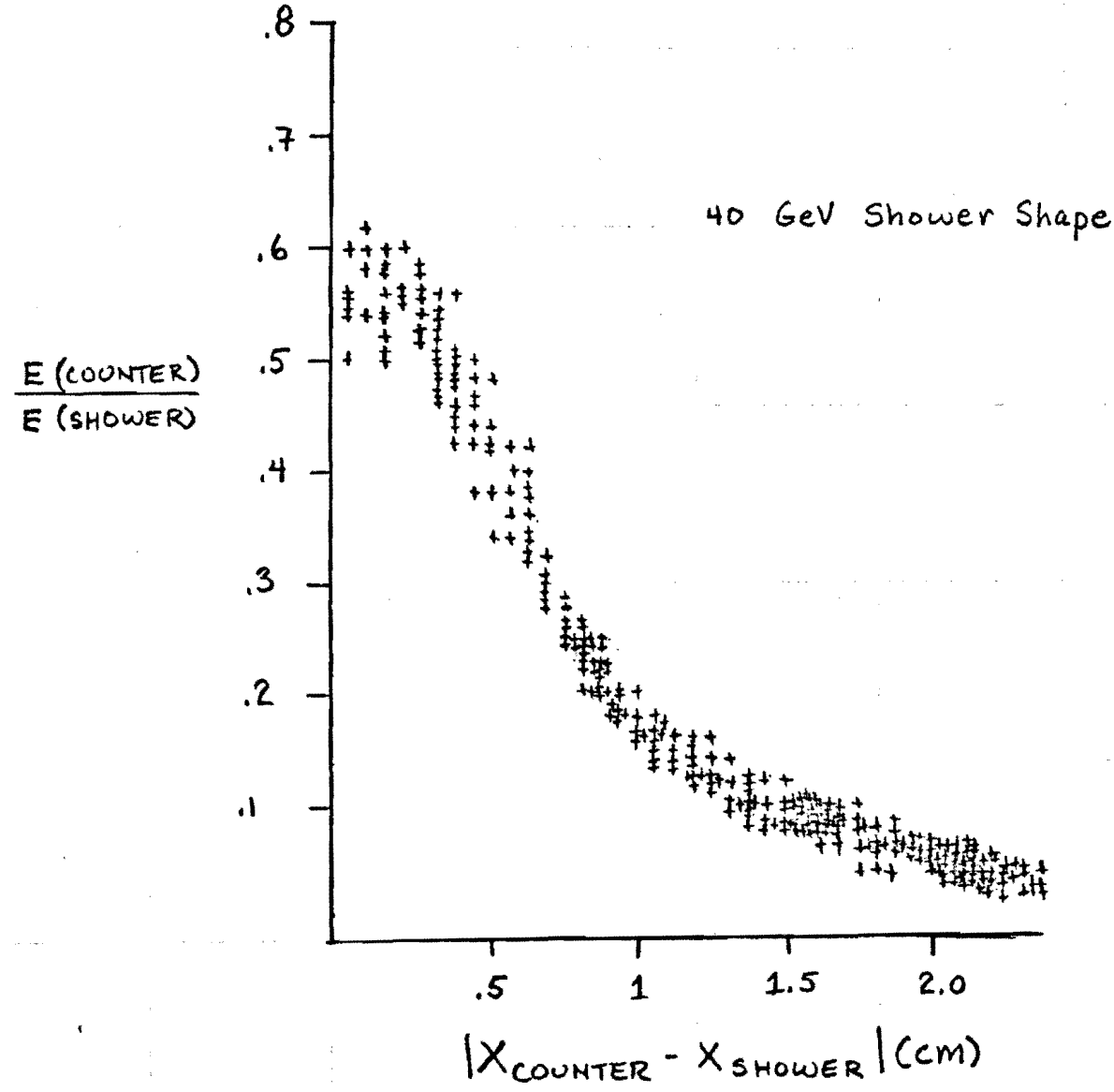

FIGURE 9

40 GeV SHOWER SHAPE

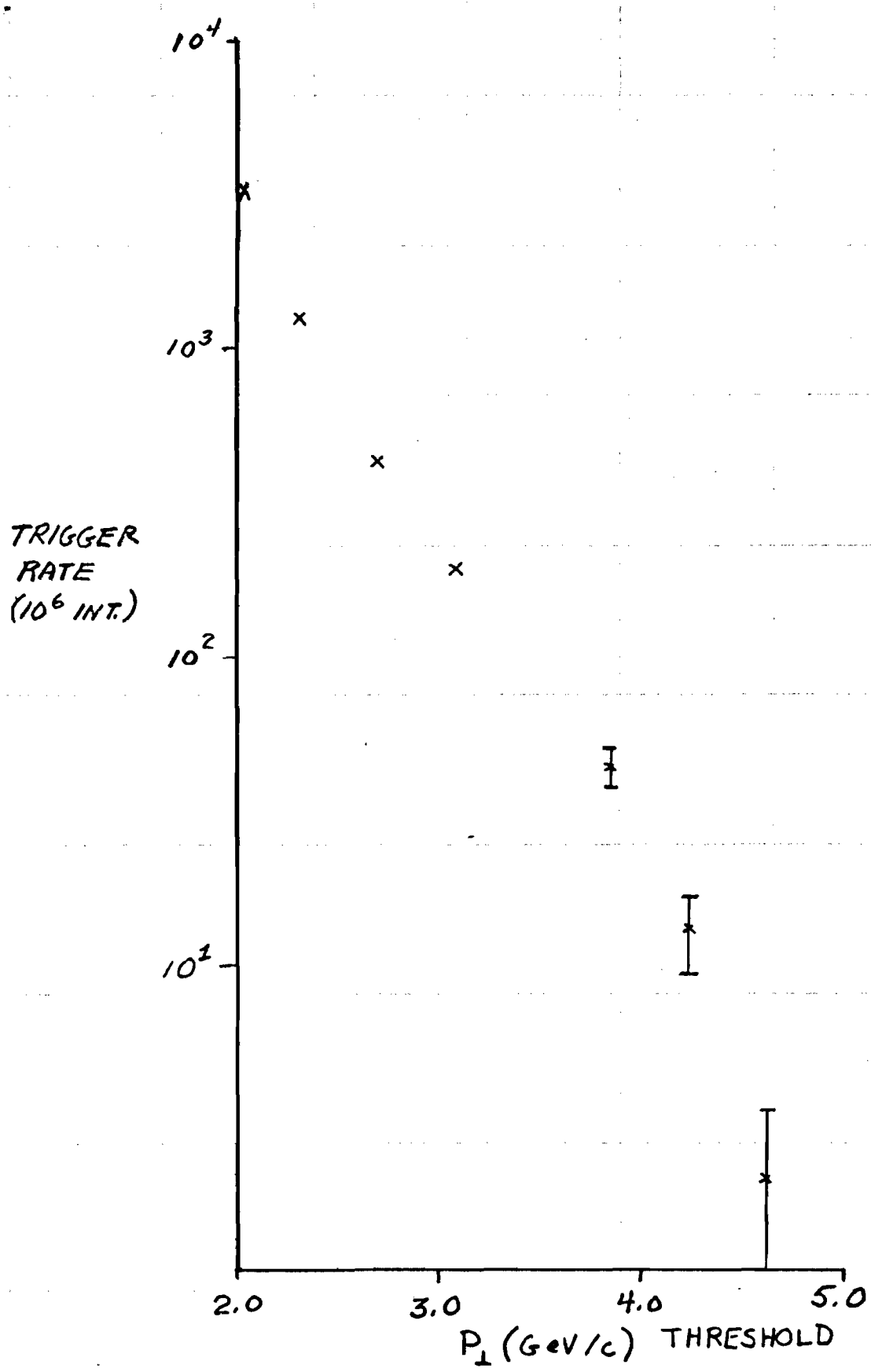
10^4
10^3
10^2
10^1
TRIGGER RATE (10^6 INT.)
2.0
3.0
4.0
5.0
$P_\perp$ (GeV/c) THRESHOLD

FIGURE 10

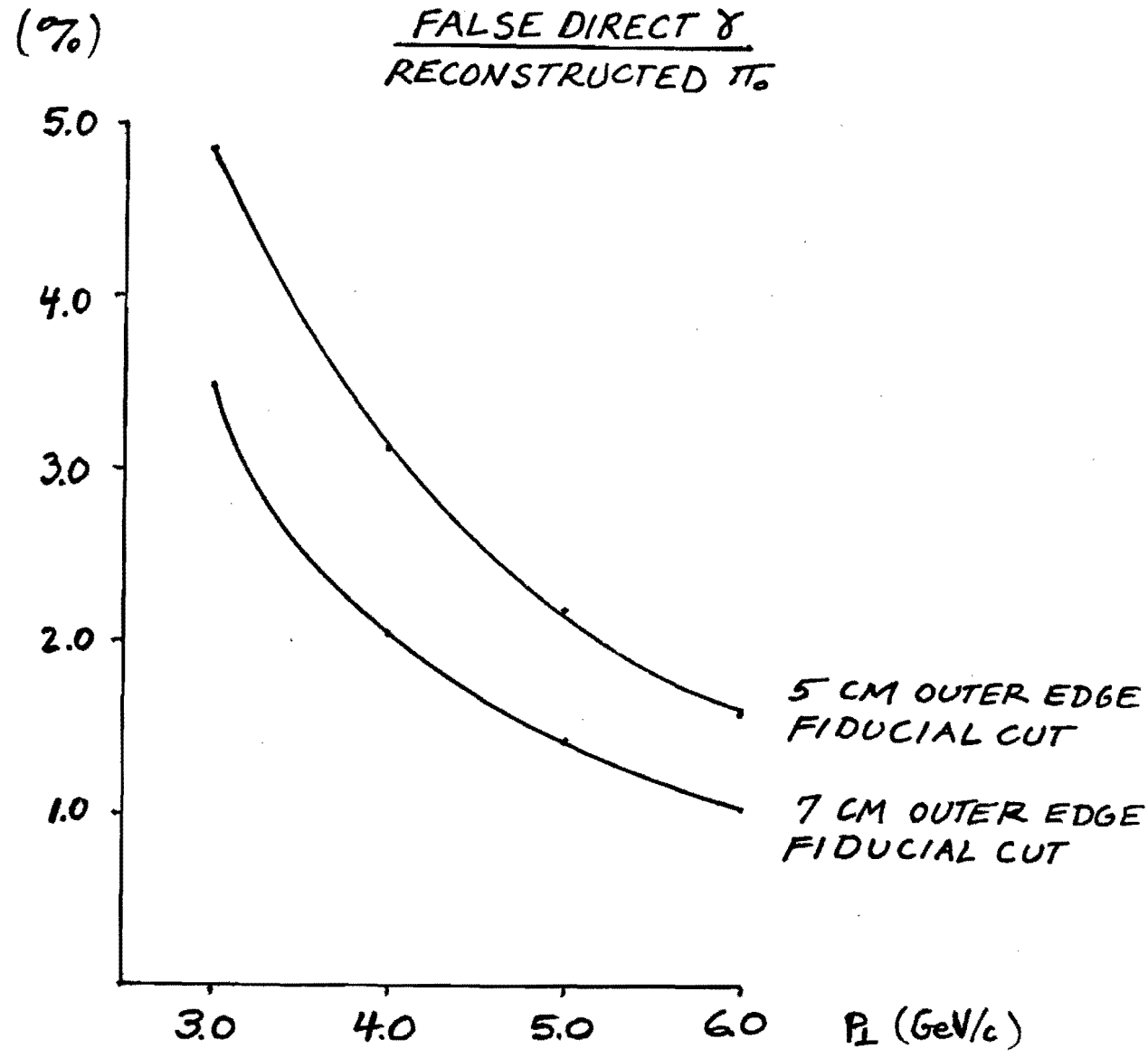
(%)
FALSE DIRECT γ
RECONSTRUCTED π₀
5.0
4.0
3.0
2.0
1.0
5 CM OUTER EDGE
FIDUCIAL CUT
7 CM OUTER EDGE
FIDUCIAL CUT
3.0
4.0
5.0
6.0
P_L (GeV/c)

FIGURE 11

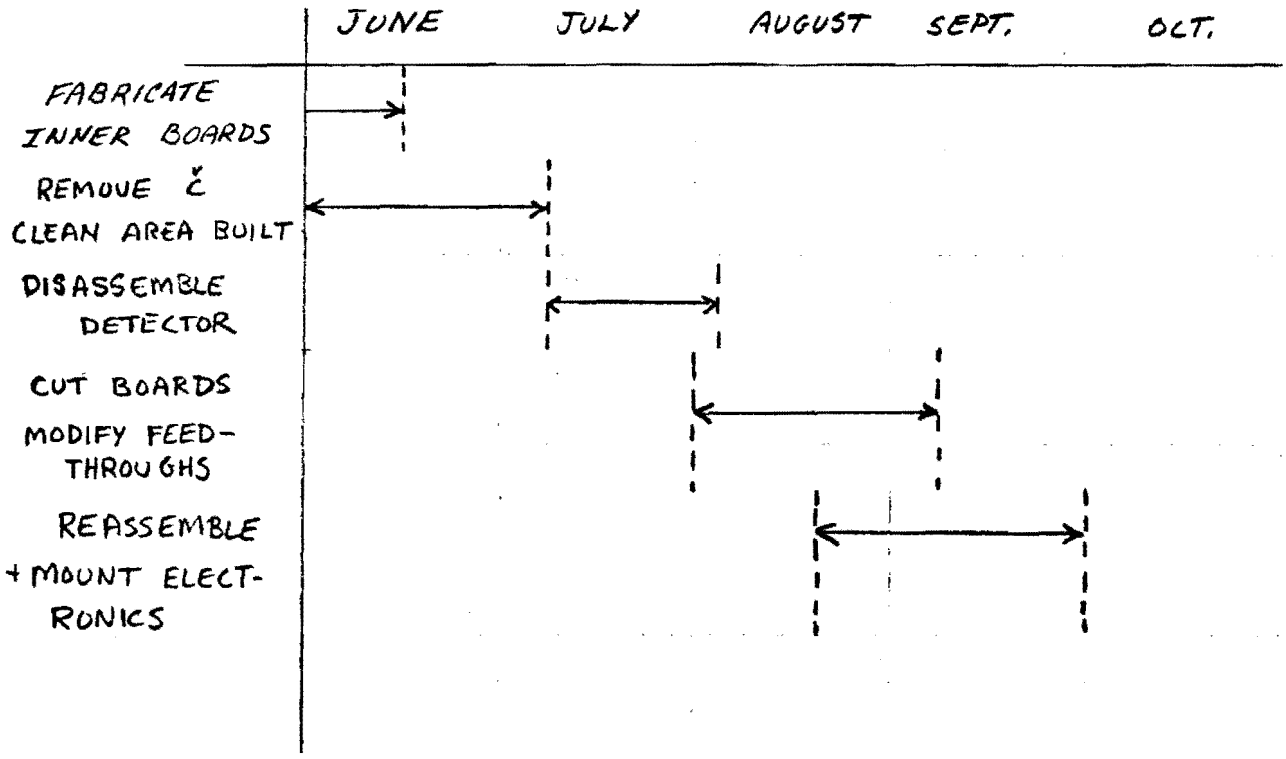

NO PLUMBING CHANGES
NO STRUCTURAL CHANGES

FIGURE 12

SHOWER DETECTOR MODIFICATION SCHEDULE

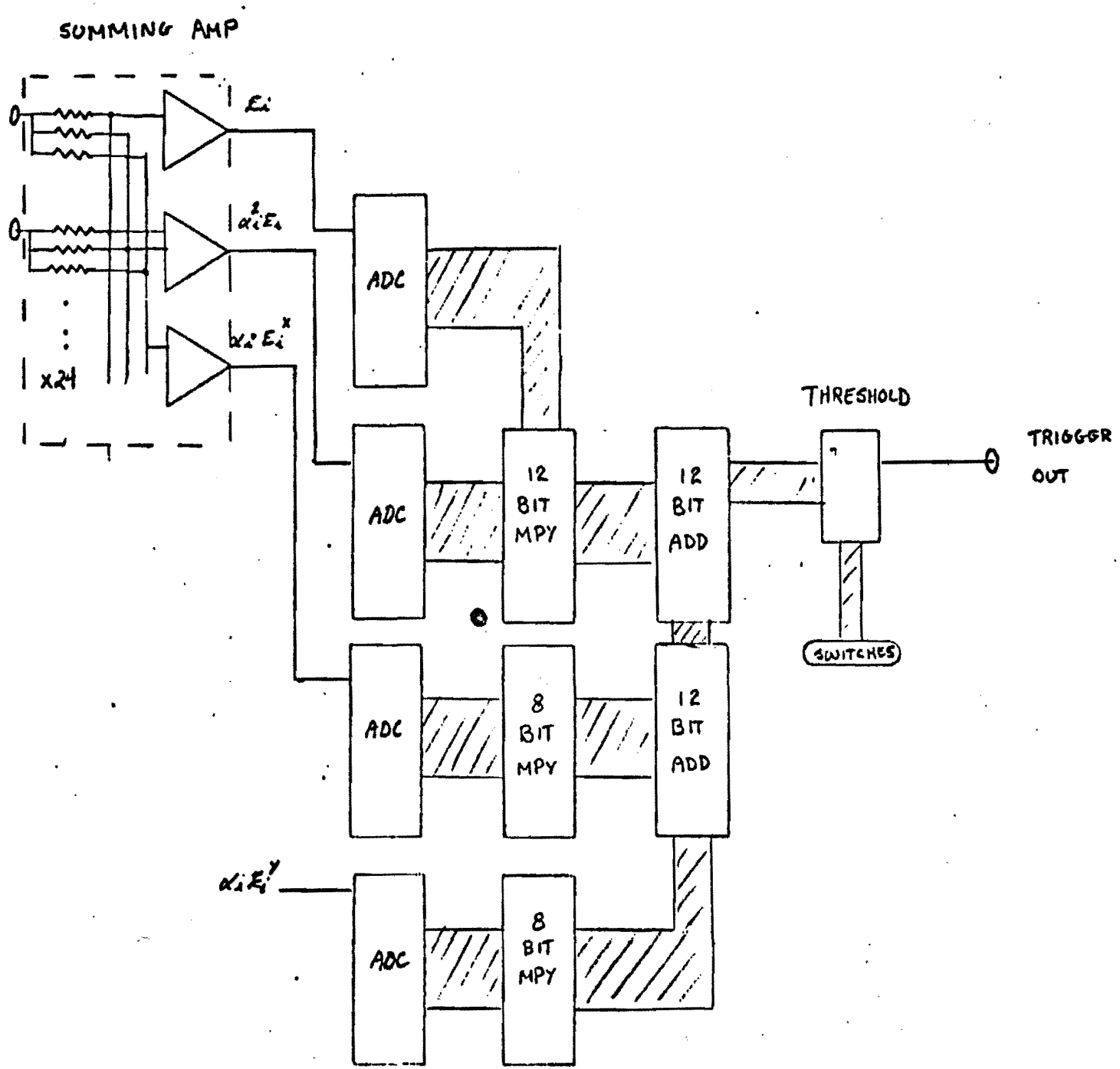
SUMMING AMP
E_i
$\alpha_i^2 E_i$
$\alpha_i E_i^x$
x24
ADC
ADC
ADC
ADC
12 BIT MPY
8 BIT MPY
8 BIT MPY
12 BIT ADD
12 BIT ADD
THRESHOLD
TRIGGER OUT
SWITCHES
$\alpha_i E_i^y$

FIGURE 13

APPENDIX I

THE P614 MASS TRIGGER

The study of high P_t processes and high mass states has become increasingly important in high energy physics. Such experiments require the state-of-the-art in detectors and fast triggering logic to select these rare interactions from low mass--low P_t interactions, which typically occur several orders of magnitude more frequently. One such area which has never been effectively explored is the subject of high mass multi-photon states. What is required are large shower detectors with good spatial and energy resolution, large active area, and high rate capability. This is achieved in the new generation of large liquid argon ion chambers. We have built a triggering system for the E515 argon calorimeter designed to select events of high mass or large P_t and capable of examining these events at a rate of 5 MHz.

The liquid argon detector built for E515 has a sensitive area of 1.2 meters x 2.4 meters. It is segmented into 1.2 cm strips in both x (vertical strips) and y (horizontal strips) as well as into front and back halves. Each four strips are summed to provide a fast output (a total of 48 x and 48 y outputs). These analog outputs provide the total energy deposited in the segments and are used for debugging and triggering the detector. The total rate capability is determined by the electron drift

time in the 2 mm argon gap. With 1% methane added to the liquid argon, the typical drift time is 175ns. Each strip in the detector is digitized using sample/hold circuitry and a single 10 bit ADC. This sample/hold circuitry requires a trigger within 600ns of the interaction and then takes approximately 1MS to read out the entire chamber.

In the limit of small particle masses, one can write the total mass of a multi-particle system as:

$$(\text{mass})^2 = M_0 M_2 - (M_1^x)^2 - (M_1^y)^2$$

$$M_0 = \sum E_i$$

$$M_1^{x,y} = \sum a_i^{x,y} E_i$$

$$M_2 = \sum ((a_i^x)^2 + (a_i^y)^2) E_i$$

Where a_i is the angle of emission of the i'th particle. Our calorimeter can provide measurements of the total electromagnetic energy in an event as well as (due to the segmentation) its moments ($M_{0,1,2}$). The principle behind the mass trigger is to calculate the moments using an analog summing amplifier, digitize them using flash digitizers, and complete the calculation using digital arithmetic elements. The entire calculation is done by the mass trigger in less than 400ns.

The analog section consists of four 24 input fast summing amplifiers. Each input is fed into each of 3 summing junctions through a weighting resistor. The weights can be set by plugging

in the appropriate set of resistors. In addition, a portion of the total energy sum is subtracted from the first and second moments to compensate for induced positive pulses due to the finite bypass capacitance of the detector.

A schematic of the digital section is shown in Figure 13. Four TRW 8 bit ADC's are used to digitize the moments. The outputs of the ADC's are then fed into digital multipliers which perform the first part of the calculation. Because the overall scale of the zeroth moment ($\sum E_i$) is much larger than the first and second moments, the analog gains of the second and third moments are set a factor of 8 higher than the 0'th moment. These are then shifted into the arithmetic elements. With most of the calculations done in parallel, the final mass squared is available within approximately 375ns of the pre-trigger input. This digital output is compared with a threshold set on the front panel, and a trigger is generated if the threshold is exceeded. Because of its pipeline construction the entire unit can operate at a rate of approximately 10 MHz. This means that every interaction or subset of interactions can be examined.